Chapter 2

Theory and Literature Review

Composites make up a very broad and important class of engineering materials [6, p. 1]. The increasing usage of these materials is spreading worldwide as a result of a large investment in the technology over the last two or more decade. Composites are used in a variety of applications. Furthermore, there is considerable scope for tailoring their structure to suit the service condition. This concept is well illustrated by biological materials such as wood, bone, teeth and hides. These materials are natural composites with complex internal structures designed to give mechanical properties well suited to the performance requirement. Today, the use of composites in structures of all kinds is accelerating rapidly, with the major impact already being felt in the aerospace industry where the use of composites has directly enhanced the capability of fuel-efficient aircraft [7, p. 1]. Adaptation of manufactured composite structures for different engineering purposes requires input from several branches of science. In this chapter, an overview of the composites in particular the polymer composites aspect including polymer surface modification techniques are highlighted..

2.1 What are Composites?

There is no exact definition of composites. The Microsoft Encarta dictionary 2003 defines a composite as something made from different parts. The difficulty in defining a composite is the size limitation on the constituents which make up the material. At the atomic level metal alloys and polymeric materials could be called composites since they consist of different and distinct atomic groupings. At the microstructure level (about 10^{-6} to 10^{-4}m) polymer blends could be called composites since their blended components are distinctly visible constituents as observed in the microscope. At the macrostructure level (about 10^{-4} to 10^{-2}m or greater) a glass-fiber-reinforced plastic, in which the glass fibers can be distinctly recognized by the naked eye, could be considered a composite.

In engineering design, however, a composite usually refers to a material consisting of constituents in the micro-macrosize range, and even favors the macrosize range. For the entire of this thesis book, the following is a definition for a composite:

"Composite is a materials system composed of a mixture or combination of two or more micro- or macroconstituents that differ in form and chemical composition and which are essentially insoluble in each other" [8, p. 590].

2.2 Types of Composite Material

According to the above definition, many materials can be classified as composites. This is particularly true for natural biological materials, which are often made up of at least two constituents. In many cases, a strong and stiff component presented often in an elongated form is embedded in a softer constituent forming the ***matrix***. For example, wood is made up of fibrous chains of cellulose molecules in a matrix of lignin, while bone and teeth are both essentially composed of hard inorganic crystals (hydroxyapatite or osteones) in a matrix of a tough organic constituent called collagen.

There are several different types of composites. According to the nature of the matrix, three major classes of composites, polymer matrix composites (PMCs), metal matrix composites (MMCs), and ceramic matrix composites (CMCs), can be categorized. Most composites in industrial use are based on polymer matrices; thermosets and thermoplastics. Since they have found wide spread applications, can be fabricated in to large and complex shapes. In addition, PMCs have been accepted in a variety of aerospace and commercial applications.

2.3 Polymer Matrix Composite

Polymer composites are consisted of components such as particles or fibers (reinforcement) bound together by an organic polymer (matrix).These reinforced plastics are a synergistic combination of reinforcement and matrices. Fibrous composite materials typically have two or more distinct phases, which include high strength/stiffness reinforcing fibers and the encapsulating matrix material. Fibers can be either discontinuous (chopped) or continuous.

Polymer matrices typically fall into two categories: thermoplastic and thermosetting polymers. Thermoplastic polymers are distinguished by their ability to be reshaped upon appropriated heating (above the glass transition temperature of the amorphous phase or the melting temperature of the crystalline phase). This cycle can be carried out repeatedly. Thermosetting polymers, on the other hand, undergo chemical reactions during curing which crosslink the polymer molecules. Once crosslinked, thermosets become

permanently hard and simply undergo chemical decomposition under the application of excessive heat. Thermosetting polymers typically have greater abrasion resistance and dimensional stability over those of thermoplastic polymers, which typically have better flexural and impact properties.

The development of PMCs for structural applications started in the 1950s; and they are by far the most common fiber reinforced composite materials in use today. One reason for their growing use is that their processing is relatively simple and does not require very high temperatures and pressures. The equipment required for processing PMCs is also relatively simple and less expensive than that required for other types of composites. There are also a variety of processing techniques available for producing PMCs parts. Depending on the type of PMCs used, some of these techniques can be highly automated.

The most significant advantage of PMCs derives from the fact that they are lightweight materials with high strength and modulus values. The light weight of PMCs is due to the low specific gravities of their constituents. Polymers used in PMCs have specific gravities between 0.9 and 1.5, and the reinforcing fibers have specific gravities between1.4 and 2.6. Depending on the types of fiber and polymer used and their relative volume fraction, the specific gravity of a PMC is between1.2 and 2, compared to 7.87 for steel and 2.7 for aluminum alloys. Because of their low specific gravities, the strength-to-weight and modulus-to-weight ratios of PMCs are comparatively much higher than those of metals and their composites (Table 2.1). Although the cost of PMCs can be higher than that of many metals, especially when carbon or boron fibers are used as reinforcements, their cost on a unit volume basis can be competitive with that of the high performance metallic alloys used in aerospace industry.

Table 2.1 Comparative properties of metal and polymer matrix composite[a] [9, p. 13]

Material	Density (g/cm^3)	Modulus (GPa)	Tensile Strength (MPa)	Yield strength (MPa)	Modulus To weight ratio (10^6 m)	Tensile Strength to weight ratio (10^6 m)	Elongation (%)
SAE 1010 steel (cold drawn)	7.87	207	368	302	2.68	4.72	20
AISI 4340 steel (quenched and tempered)	7.87	207	1722	1515	2.68	22.3	-
6061-T6 aluminum alloy	2.70	68.9	310	275	2.60	11.7	15
7075-T6 aluminum alloy	2.70	68.9	571	503	2.60	21.6	11
AZ80A-T5 magnesium alloy	1.74	44.8	379	276	2.02	22.2	7
Ti-6Al-4V titanium alloy (aged)	4.43	110	1171	1068	2.53	26.9	8
High-strength carbon fiber/epoxy (unidirectional)	1.55	138	1550	-	9.07	101.9	1.1
High-modulus carbon fiber/epoxy (unidirectional)	1.63	215	1340	-	13.44	77.5	0.6
E-glass fiber/epoxy (unidirectional)	1.85	39.3	965	-	2.16	53.2	2.5
Kevlar 49/epoxy (unidirectional)	1.38	75.8	1378	-	5.60	101.8	1.8
Carbon fiber/epoxy (quasi-isotropic)	1.55	45.5	579	-	2.99	38.14	-
E-glass fiber/epoxy (random fiber SMC)	1.87	15.8	164	-	0.86	8.9	1.73

[a]For unidirectional composites, the modulus and strength values are in fiber direction.

A second advantage of PMCs is the design flexibility and the variety of design options that can be exercised with them. Fibers in a PMCs can be selectively placed or oriented to resist load in any direction, thus producing directional strength or moduli instead of equal strength or modulus in all directions as in isotropic materials such as metals and unreinforced polymer. Similarly, fiber type and orientation in a PMC can be controlled to produce a variety of thermal properties such as the coefficient of thermal expansion. PMCs can be combined with aluminum honeycomb, structural plastic foam, or balsa wood to produce sandwich structures that are stiff and at the same time lightweight. Two or more different types of fibers can be used to produce a hybrid construction with high flexural stiffness and impact resistance.

There are several other advantages of PMCs that make them desirable in many applications. They have damping factors that are higher than those of metals, which means that noise and vibrations are damped in PMC structures more effectively than in metal structure. They also do not corrode. However, depending on the nature of the matrices and

fibers, their properties may be affected by environmental factors such as elevated temperatures, moisture, chemical, and ultraviolet light.

An important point to note is that, unlike ductile metals such as low-carbon steel and wrought aluminum alloys, PMCs do not exhibit gross yielding. For many PMCs, the stress-strain diagram can be nonlinear; however, the nonlinearity is not due to plastic deformation as is observed in ductile metals. The nonlinear behavior of PMCs is due to a number of types of microscopic damage such as fiber breakage, matrix cracking, fiber/matrix interfacial debonding, and delamination, which can occur at relatively low stress. These damages grow in size as well as in number at various locations in the PMC as the stresses are increased. There may not be an immediate failure; however, the stiffness of the material is progressively decreased. In most PMCs, high stresses at holes of cutouts are reduced by the initiation of these damages, reducing the notch sensitivity of the material.

2.4 Fiber Architecture

Many composite properties are strongly dependent on the arrangement and distribution of fibers so called the fiber architecture. This expression encompasses intrinsic features of the fibers, such as their diameter and length, as well as the volume fraction of the fibers and their alignment and packing arrangement. Figure 2.1 gives several examples of the possible composite reinforcement forms.

In the linear form, the fibers can be either continuous or discontinuous. Continuous fibers are used in filament wound, pultruded, or laminated structures in which the fiber orientation can be precisely controlled. Discontinuous fibers are either directly mixed with the matrix, for example in injection-molded structures, or combined with a binder to form a planar mat. In these cases, there is very little control over the fiber orientation.

Two- and three-dimensional architectures are produced by means of textile processes such as interlacing, intertwining and interloping continuous fiber in textile machines. These processes provide good control over the fiber orientation as well as fiber placement and can be used to produce a variety of complex shapes or preforms, in a relatively short time. Two-dimensional architecture is used in laminated structures. Three-dimensional arrangement of continuous fibers is used when interlaminar failure or delamination becomes a problem. The use of continuous fibers in the thickness direction improves the interlaminar fracture toughness. Three-dimensional architecture can also be used to build composites with nearly isotropic.

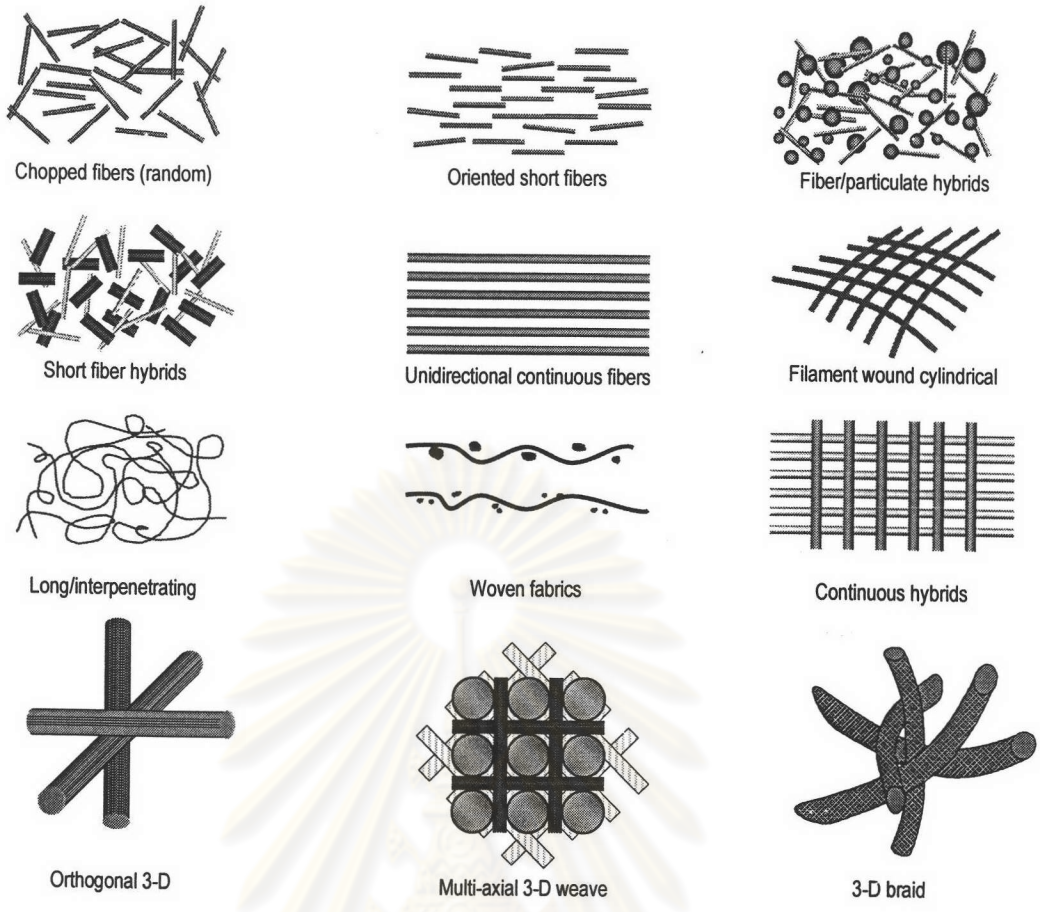

Figure 2.1 Examples of reinforcement styles, combinations, orientations and configurations [redrawn from ref. 10, p.4]

2.4.1 Volume Fraction and Weight Fraction

An important parameter controlling the properties of a fiber reinforced composite material is the fiber volume fraction. Although most calculations on composite materials are based on the volume fractions of the constituents, it is sometimes important, particularly when calculating the density of the composite, to use weight fractions. The appropriate conversion equations are:

$$V_f = \frac{W_f / \rho_f}{W_f / \rho_f + W_m / \rho_m} \tag{2.1}$$

and

$$W_f = \frac{V_f \rho_f}{V_f \rho_f + V_m \rho_m} \tag{2.2}$$

where V_f, V_m are volume fractions, W_f, W_m are weight fractions and ρ_f, ρ_m are densities of the fiber and matrix, respectively. For ideal regular hexagonal close packing of

fibers of circular cross-section, i.e. when the fibers just touch, the volume fraction of fibers would reach the value of 0.91 and for ideal regular square close packing the value of volume fraction would be 0.76. In practice, very large bundles or tows of fibers are aligned mechanically and the ideal distribution is only realized in small localized regions. Fiber bunching and matrix-rich areas occur. Values of V_f greater than 0.65 are difficult to achieve.

2.4.2 Fiber Orientation Angle

Another important parameter controlling the properties of a fiber reinforced composite material is the fiber orientation angle, which defined the orientation of fibers with respect to the loading directions (Figure 2.2). The fiber orientation angle is commonly defined using right-handed coordinate systems.

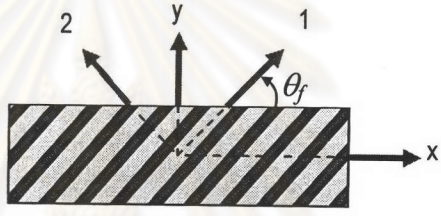

Figure 2.2 Fiber orientation angle on a lamina [redrawn from ref. 9, p.5]

In uniaxial tensile loading, fibers are most effective when they are oriented parallel to the loading direction, the fiber orientation angle, θ_f, is 0°. However, in pure shear loading, the fibers are most effective when they are oriented at +45° and -45° angles with respect to loading axis. In Figure 2.3, plots of experiment data and prediction from calculation of the modulus against the fiber orientation angle are shown.

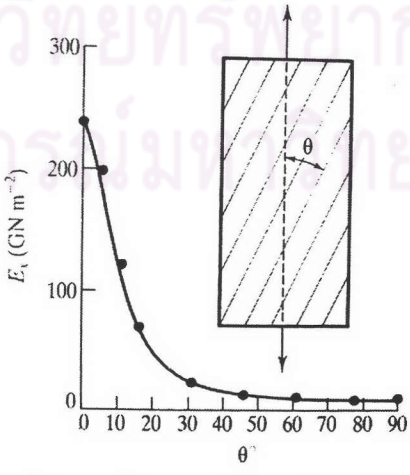

Figure 2.3 The angular dependence of the modulus of a unidirectional CFRP (carbon fiber reinforced plastic) lamina (V_f = 0.5). The continuous line is the prediction from calculation. The points are experimental values. Redrawn from data given by Hull [11, p.223]

2.5 The Concept of Load Transfer [6, p.6-7]

Central to an understanding of the mechanical behavior of a composite is the concept of load sharing between the matrix and the reinforcing phase. The stress may vary sharply from point to point (particularly with short fibers or particles as reinforcement), but the proportion of the external load borne by each of the individual constituents can be gauged by volume-averaging the load within them. At equilibrium, the external load must equal the sum of the volume-averaged loads borne by the constituents (e.g. the matrix and the fiber). This gives rise to the condition

$$V_f\overline{\sigma}_f + (1 - V_f)\overline{\sigma}_m = \sigma_A \tag{2.3}$$

governing the volume-averaged matrix and fiber stresses ($\overline{\sigma}_m$, $\overline{\sigma}_f$) in a composite under an external applied stress σ_A , containing a volume fraction V_f of reinforcement. For a simple two-constituent composite under a given applied load, a certain proportion of that load will be carried by the fiber and the remainder by the matrix. Provided the response of the composite remains elastic, this proportion will be independent of the applied load and it represents an important characteristic of the material. It depends on volume fraction, shape and orientation of the reinforcement and on the elastic properties of both constituents.

2.6 Elastic Deformation of Unidirectional Continuous Fiber Composites

Clearly the properties of the unidirectional composite (Figure 2.4) will be highly anisotropic since all fibers are aligned in one direction. For example, strength, stiffness, thermal expansion and conductivity properties will be different in directions parallel and perpendicular to the fibers.

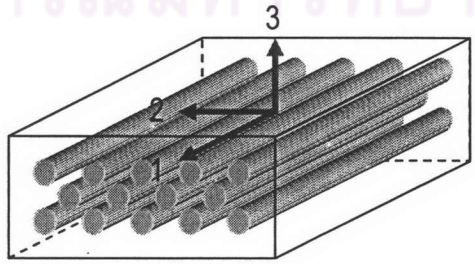

Figure 2.4 Model of unidirectional continuous fiber composite.

2.6.1 Axial Stiffness (Isostrain Condition)

A unidirectional continuous fiber composite can be treated as it was composed of parallel slabs of the two constituents bonded together, with relative thickness in proportion to the volume fractions of matrix and fiber. This is illustrated in Figure 2.5. The two slabs are constrained to have the same lengths parallel to the bonded interface. Thus if a stress is applied in direction of fiber alignment (the 1-direction), both constituents exhibit the same strain in this direction, ε_1 [6, p.61]. This 'equal strain' condition is valid for loading along the fiber axis, provided that there is no interfacial sliding. The detailed nature of the interfacial region and the consequences of the imperfect bonding are considered in next section.

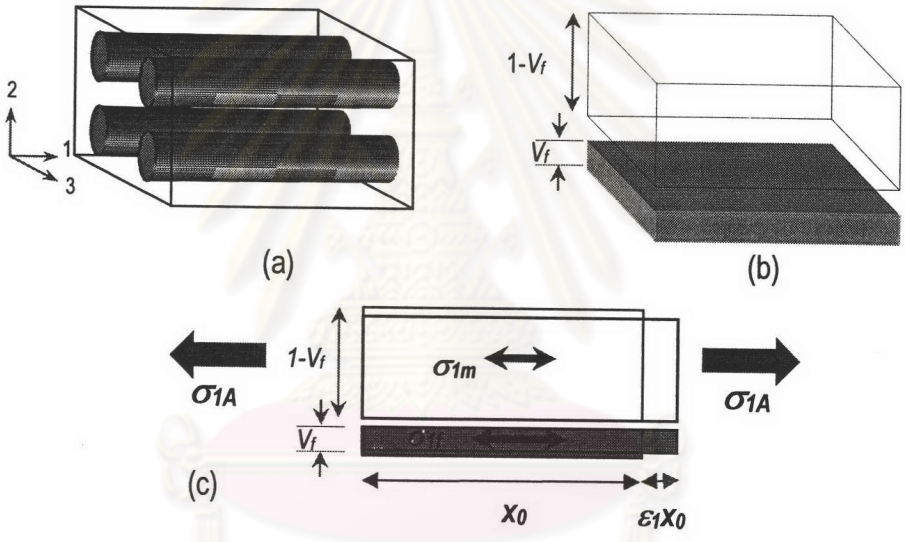

Figure 2.5 Schematic illustration of (a) a composite containing a volume fraction V_f of aligned, continuous fibers, and (b) a representation of this as bonded slabs of matrix and fiber material. (c) On applying a stress σ_{1A} parallel to the fiber axis, the two slabs experience the same axial strain ε_1 [redrawn form ref. 6, p.61].

It is now a simple matter to derive Young's modulus of the composite, E_1. The axial strain in the fiber and the matrix must correspond to the ratio between the stress and the Young's modulus for each of the two components, so that

$$\varepsilon_1 = \varepsilon_{1f} = \frac{\sigma_{1f}}{E_f} = \varepsilon_{1m} = \frac{\sigma_{1m}}{Em} \qquad (2.4)$$

The overall stress σ_{1A} can be expressed in terms of two contributions being made

$$\sigma_{1A} = (1-V_f)\sigma_{1m} + V_f\sigma_{1f} \tag{2.5}$$

The Young's modulus of the composite can now be written

$$E_1 = \frac{\sigma_{1A}}{\varepsilon_1} = \frac{[(1-V_f)\sigma_{1m} + V_f\sigma_{1f}]}{(\sigma_{1f}/E_f)} = E_f\left[\frac{(1-V_f)\sigma_{1m}}{\sigma_{1f}} + V_f\right]$$

Using the ratio between the stresses in the components given by Equation 2.4, this simplified to

$$E_1 = (1-V_f)E_m + V_fE_f \tag{2.6}$$

This well known 'Rule of Mixture' indicates that the composite stiffness is simply a weighted mean between the moduli of the two components, depending only on the volume fraction of the fibers. Accurate experimental validation of the rule of mixtures has been demonstrated for a number of composites with continuous fibers.

2.6.2 Transverse Stiffness (Isostress Condition)

The conventional approach is to assume that the system can again represented by the 'slab model' depicted in Figure 2.6. In the fiber composite shown in Figure 2.4, both 2- and 3-directions are transverse to the fibers. For this analysis the isotropic properties in 2- and 3-directions are assumed, i.e. $E_2 = E_3$. A more questionable assumption is that transverse stress on the composite is the same in the fiber and matrix, i.e. $\sigma_{2A} = \sigma_{2f} = \sigma_{2m}$, and the strains can be expressed in terms of the applied stress. The overall net strain can be written as

$$\varepsilon_2 = V_f\varepsilon_{2f} + (1-V_f)\varepsilon_{2m} \tag{2.7}$$

from which the composite modulus is given by

$$E_2 = \frac{\sigma_{2A}}{\varepsilon_2} = \frac{\sigma_{2A}}{[V_f\varepsilon_{2f} + (1-V_f)\varepsilon_{2m}]}$$

Substituting expressions for $\varepsilon_{2f} = \sigma_{2f}/E_f, \varepsilon_{2m} = \sigma_{2m}/E_m$ and $\sigma_{2A} = \sigma_{2f} = \sigma_{2m}$ gives

$$\frac{1}{E_2} = \frac{V_f}{E_f} + \frac{(1-V_f)}{E_m} \tag{2.8}$$

The isostress treatment is often described as a 'Reuss model' or 'inverse rule of mixture'.

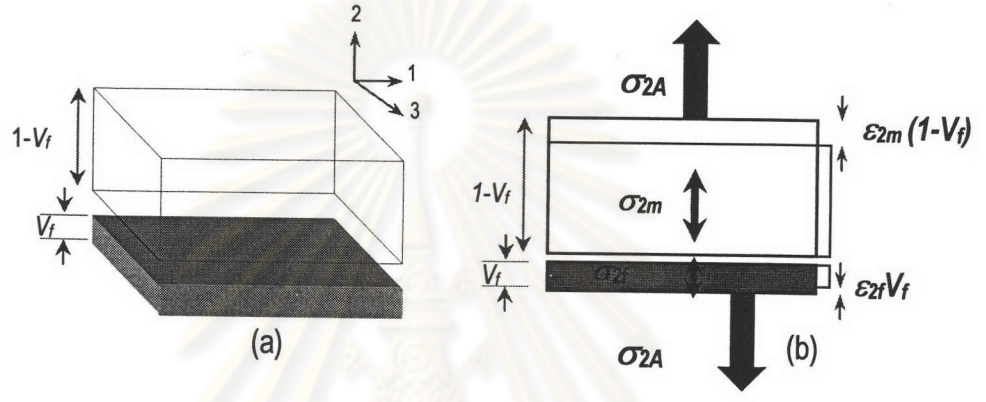

Figure 2.6 Schematic showing (a) the slab model and (b) the isostress assumption during transverse stressing [redrawn from ref. 6, p.63].

However, Equation (2.8) gives a poor approximation for E_2. The true nature of the stress and strain distributions during this type of loading was provided by the technique of photoelasticity. The photoelastic image shows the non-uniform distribution of stress and strain during transverse loading. This means the isostress condition is inadequate. In 1967, Halpin and Tsai proposed more accurate estimates, which is not based on rigorous elasticity theory, but broadly takes account of enhanced fiber load bearing, relative to the isostress assumption. Their expression for transverse stiffness is

$$E_2 = \frac{E_m(1+\xi\eta V_f)}{(1-\eta V_f)} \tag{2.9}$$

in which

$$\eta = ((E_f/E_m)-1)/((E_f/E_m)+\xi)$$

The value of ξ may taken as an adjustable parameter, but its magnitude is generally of the order of unity. The expression gives good agreement with experiment over the complete range of fiber content. A comparison is presented in Figure 2.7 between the predictions of Equation (2.6), (2.8) and (2.9) and experimental data for a glass/polyester system. It is clear that the isostrain treatment (Equation (2.6)) is in close agreement with data for axial modulus. For the transverse modulus, both isostress and Halpin-Tsai treatments (Equation (2.8) and (2.9)) is less clear. The experimental data show scatter and many of them lie closer to the isostress curve than to the Halpin-Tsai prediction. This behavior is the result of inelastic deformation of the matrix. However the Halpin-Tsai equation is generally more applicable and allow for variation in packing geometry an regularity with the factor ξ.

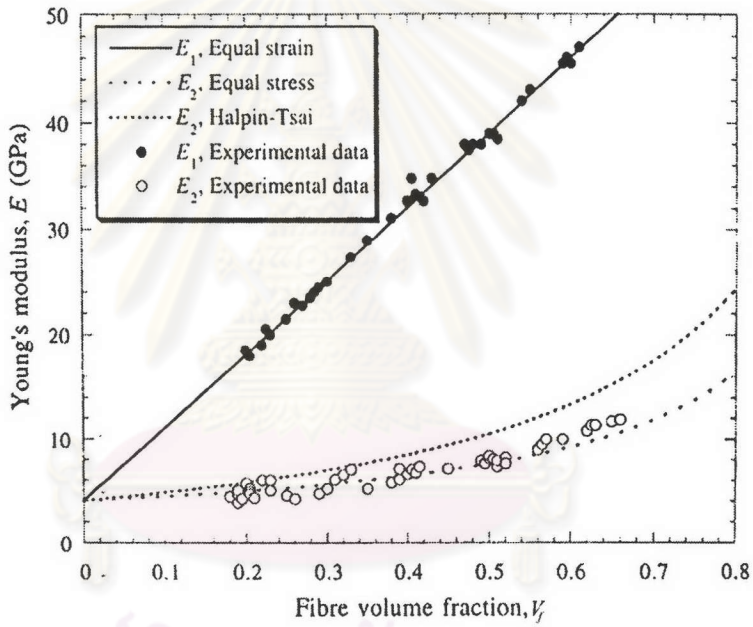

Figure 2.7 Comparison between experimental data for the axial and transverse Young's moduli, E_1 and E_2, for polyester/glass composites and corresponding predictions from the isostrain model (Equation (2.6)) for E_1 and the isostress (Equation (2.8)) and Halpin-Tsai (Equation (2.9), with $\xi = 1$) models for E_2. The experimental E_2 values have been affected by inelastic deformation of the matrix.

2.7 Interfaces

The preceding section has dealt with the elastic behavior of composite among the assumptions that the interfacial bond is 'perfect'. This means that there is no debonding, cracking or sliding – in fact, no elastic or inelastic processes of any description. In practice, many important phenomena may take place at the interface, depending on its structure and the stresses generated there. These processes tend to promote plastic deformation of the matrix and can also influence the onset and nature of failure. To consider the strength and fracture behavior of composites it is necessary to consider the interface first.

An interface between a reinforcement and a matrix can be defined as the bounding surface between the two across which a discontinuity in some parameter occurs [12, p.101]. The discontinuity across the interface may be sharp or gradual. Mathematically, interface is a bidimensional region. In practice, the interfacial region has a finite thickness. In any event, an interface is the region through which material parameters, such as concentration of an element, crystal structure, atomic registry, elastic modulus, density, coefficient of thermal expansion and etc., change from one side to another. Clearly, a given interface may involve one or more of these items.

The behavior of a composite material is a result of the combined behavior of the following three entities:

- Fiber or reinforcing constituent
- Matrix
- Fiber/matrix interface

The reason the interface in a composite is of great importance is that the internal surface area occupied by interface is quite extensive. Specifically, in the case of fiber reinforced composite, the internal surface area can be as high as 3000 cm^2/cm^3 with a reasonable fiber volume fraction.

The reinforcement is effective in strengthening the matrix only if a strong interfacial bond exists between the reinforcement and matrix. The interfacial properties also influence the resistance to crack propagation in a composite and therefore its fracture toughness. The two most important energy-absorbing failure mechanisms in a fiber reinforced composite are debonding at the fiber/matrix interface and fiber pull out (Figure 2.8). If the

interface debonds relatively easily, the crack propagation is interrupted by the debonding process and instead of moving through the fiber, the crack moves along the fiber surface, allowing the fiber to carry higher loads. Fiber pull-out occurs because fibers do not all break at the crack plane. Since they break at random locations away from the crack plane, one of the broken fiber ends pulls out from the crack face open up with increasing load. If the pull-out occurs against high frictional forces or shear stress at the interface there may be a significant increase in fracture toughness of the composite.

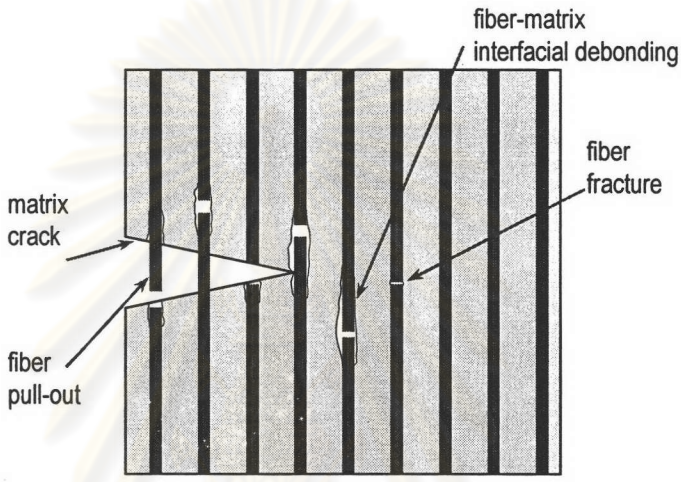

Figure 2.8 Debonding, fiber fracture and fiber pull-out in a unidirectional continuous fiber composite [redrawn from ref. no. 9 p. 10].

2.7.1 Wetting

If the surfaces of two bodies spontaneously come into intimate (atomic scale) contact when they are brought close to each other (commonly with one of the bodies in liquid form), then wetting is said to have taken place. The occurrence of wetting can be treated using simple thermodynamics, but in practice there may be chemical changes taking place which are time-dependent.

At a free surface, atoms or molecules are not surrounded by other atoms or molecules; they have bonds or neighbors on only one side. Thus there exists an imbalance of forces at the surface that results in a rearrangement of atoms or molecules at the surface. The surface has an extra energy called 'surface energy', i.e., surface energy is the excess energy per unit area associated with the surface because of the unsatisfied bonds at the surface. The unit of surface energy is J m^{-2}. Surface energy can also define as the energy needed to create

a unit surface area. 'Surface tension' is the tendency to minimize the total surface energy by minimizing the surface area. Surface energy and surface tension are numerically equal for isotropic materials. Surface tension is generally given in units of N m^{-1}, which is the same as J m^{-2}. However this is not true for anisotropic surfaces.

Wettability is a key concept to assist or impede adhesion, which defined as the ability of liquid to spread on a solid surface. Good wettability means that the liquid (matrix) will flow over the reinforcement covering every 'bump' and 'dip' of the rough surface of the reinforcement. For adhesion to occur during the manufacture of composite, the reinforcement and the matrix must be brought into intimate contact which can be established providing the liquid is not too viscous and a thermodynamic driving force exists. The latter is commonly express in terms of surface energies, γ, so that the work of adhesion, W_a, is a simple net sum, often termed the Dupre equation

$$W_a = \gamma_{SV} + \gamma_{LV} - \gamma_{SL} \qquad (2.10)$$

In practice, measuring of the wettability of a given solid can be performed by considering the equilibrium of forces in a system consisting of a drop of liquid resting on a plane of solid surface in the appropriate atmosphere. Figure 2.9 shows the situation schematically. The liquid drop will spread and wet the surface completely only if this results in a net reduction of the system free energy. Note that a portion of solid/vapor interface is substituted by solid/liquid interface. Contact angle, θ, of a liquid on the solid interface is a convenient and important parameter to characterize wettability. Commonly, the contact angle is measured by putting a sessile drop of the liquid on the flat surface of a solid substrate. The contact angle is obtained from the tangents along three interfaces: solid/liquid, liquid/vapor and solid/vapor. The contact angle can be measured directly by a goniometer or calculated by using simple trigonometric relationships involving drop dimensions, In theory, one can use the following expression, called Young's equation

$$\gamma_{SV} = \gamma_{SL} + \gamma_{LV}\cos\theta \qquad (2.11)$$

where the subscripts *SV*, *LS* and *LV* represent solid/vapor, liquid/solid and liquid/vapor interfaces, respectively. It follows that complete wetting (θ = 0°) occurs if the surface energy of the solid is equal to or greater than the sum of the liquid surface energy and the interface surface energy. Interface surface energies are difficult to obtain (and may

influenced by chemical reaction), but they are frequently smaller than the values for the phases being exposed to air. The surface energies of fibers and matrices (liquid) are generally known and systems where the former greatly exceeds the latter are likely to wet very easily. For example, glass (γ_{SV} = 560 mJ m^{-2}) and graphite (γ_{SV} = 70 mJ m^{-2}) are readily wetted by polyester (γ_{LV} = 35 mJ m^{-2}) and epoxy (γ_{LV} = 43 mJ m^{-2}) resins, but polyethylene fibers (γ_{SV} = 31 mJ m^{-2}) are not.

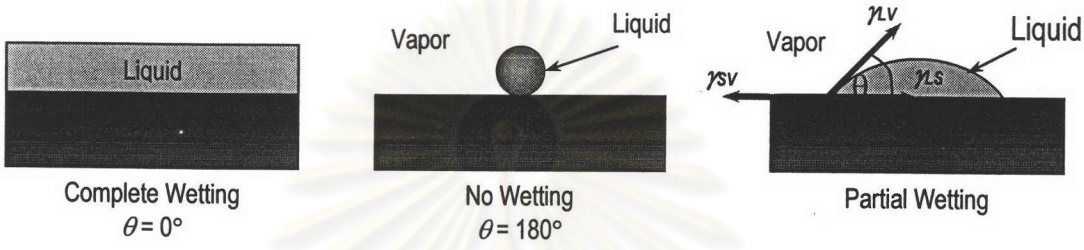

Figure 2.9 Three different conditions of wetting: complete wetting, no wetting and partial wetting. The terms γ_{SV}, γ_{LS} and γ_{LV} denote the surface energies of solid/vapor, liquid/solid and liquid/vapor interfaces, respectively. Redrawn form ref. no. 12, p.103.

Equation (2.11) is treated among the equilibrium condition which can be obtained only if the following conditions are satisfied [13, p.38].

- The surface is rigid and immobile. The vertical component of the liquid surface tension, $\gamma_{LV}\sin\theta$, is balanced by the elastic stress induced in the solid. It has been shown that deformation of low-modulus materials can lead to relative large errors. This effect becomes negligible when the Young's modulus of the material is greater than 10^5 dyne/cm^2 (10^4 Pa).
- The surface is smooth. Although there is no definite criteria for defining smoothness, surface roughness below 0.5 - 0.1μm is usually claimed to be acceptable.
- The surface is compositionally homogeneous. Compositional heterogeneity can be caused by surface contamination, migration of a low-surface-energy additive to the surface, or migration of the low-surface-energy component(s) to the surface from a polymer blend or a block copolymer.
- There are no interactions between the liquid and the solid surface.

For systems satisfying all these conditions, there is one and only one equilibrium contact angle; however, these conditions are seldom completely met for practical system. Therefore, contact angle hysteresis is a common phenomenon. It is important to point out that γ_{SV} is not the surface tension of the solid γ_S but represents the surface tension of the solid resulting from adsorption of vapor from a liquid. The value of γ_{SV} can be considerably lower than that of γ_S in vacuum. The amount of reduction in the surface tension of the solid is referred to as the spreading pressure π_S.

$$\pi_S = \gamma_S - \gamma_{SV} \qquad (2.12)$$

Combining Equation (2.11) and (2.12) yields:

$$\cos\theta = \frac{\gamma_S - \pi_S - \gamma_{SL}}{\gamma_{LV}} \qquad (2.13)$$

If the value of $\cos\theta$ for a series of homologous liquid are plotted against the surface tension of liquid, γ_{LV} , the intercept of the linear line at $\cos\theta = 1$ is the critical surface tension γ_C. The plot of $\cos\theta$ versus γ_{LV} is known as the Zisman plot. When $\cos\theta = 1$ and $\gamma_C = \gamma_{LV}$, Equation (2.12) can be written as:

$$\gamma_C = \gamma_S - (\gamma_{SL} + \pi_S) \qquad (2.14)$$

The critical surface tension values are empirically related to the surface constitution. Table 2.2 summarizes the constitution of atoms and organic radicals in solid surfaces arranged in the order of increasing value of γ_c. Table 2.3 provides a summary of the critical surface tensions and surface tensions determined by various methods for a number of polymers.

Table 2.2 Surface constitution and critical surface tension at 20 °C [13, p.41]

Surface constitution	Critical surface tension (10^{-3} N m-1)
Hydrocarbon surfaces	
–CH3 (crystal)	22
–CH3 (monolayer)	24
–CH– (	31
Fluorocarbon surfaces	
$-CF_3$	6
$-CF_2H$	15
$-CF_3$ and $-CF_2-$	17
$-CF_2-CF_2-$	18
$-CH_2-CF_3$	20
$-CF_2-CFH-$	22
$-CF_2-CH_2-$	25
$-CFH-CH_2-$	28
Chlorocarbon	
$-CHCl-CH_2-$	39
$-CCl_2-CH_2-$	40
$=CCl_2$	43

Table 2.3 Surface tension and critical surface tension of polymers at 25 °C [13, p.41]

Polymer	Surface tension 10^{-3} (N m-1)	Critical surface tension 10^{-3} (N m-1)
Polyethylene	35.7	31
Polypropylene	30.1	32
Polyisobutylene	33.6	27
Polystyrene	40.7	33
Polychloroprene	43.6	38
Poly(vinyl chloride)	42.9	39
Poly(vinylidene chloride)	45.2	40
Poly(vinyl fluoride)	37.5	28
Poly(vinylidene fluoride)	36.5	25
Polytetrafluoroethylene	23.9	19
Polyhexafluoropropylene	17.0	16
Poly(chlorotrifluoroethylene)	32.1	31
Poly(vinyl acetate)	36.5	33
Poly(methyl acrylate)	40.1	35
Poly(ethyl acrylate)	37.0	33
Poly(methyl metacrylate)	41.1	39
Poly(ethylene oxide)-diol	42.9	43
Poly(ethylene terephthalate)	42.1	43
Polycaproamide, nylon6	n/a	42
Poly(hexamethylene adipamide) nylon66	44.7	46
Poly(dimethyl siloxane)	19.9	24
Poly(methyl phenyl siloxane)	26.1	n/a

It is important to realize that wettability and bonding are not synonymous terms. Wettability described the extent of intimate contact between a liquid on a solid; it does not necessariiy mean a strong bond at the interface. One can have excellent wettability and a weak van der Waals-type low energy bond. A low contact angle, meaning good wettability, is a necessary but not sufficient condition for strong bonding.

Wettability is very important in polymer matrix composites because in PMC manufacturing the liquid matrix must be penetrated and wet fiber tows. Among polymeric resins that commonly used as matrix materials, thermoset resins have a viscosity in the 1-10 Pa s range. The melt viscosities of thermoplastics are two to three orders of magnitude higher than those of the thermoset and they show, comparatively, poorer fiber wetting characteristics and poorer composites. Although the contact angle is a measure of wettability, its magnitude will depend on the following important variables: time and temperature of contact; interfacial reaction; stoichiometry, surface roughness and geometry; heat of formation and electronic configuration.

2.7.2 Types of Bonding at the Interface

To control the degree of bonding between the matrix and the reinforcement, it is necessary to understand all the different possible bonding types, one or more of which may acting at any given instant. The important types of interfacial bonding are classified as follows:

- Mechanical bonding
- Physical bonding
- Chemical bonding
    - Dissolution bonding
    - Reaction bonding

2.7.2.1 Mechanical Bonding

Simple mechanical keying or interlocking effects between two surfaces can lead to considerable degree of bonding. Primary factors controlling this type of bonding are fiber surface roughness, porosity, surface morphology, and matrix pore-filling capabilities. Any contraction of the matrix onto a central fiber would result in gripping of the fiber by the matrix. For example, a situation in which the matrix in a composite radially shrinks more than the fiber on cooling from a high temperature. This would lead to a gripping of the fiber by the matrix

even in the absence of any chemical bonding (Figure 2.10). The matrix penetrating the crevices on the fiber surface, by liquid or viscous flow or high-temperature diffusion, can also lead to some mechanical bonding. In Figure 2.10, the radial gripping stress, σ_r, related to the interfacial shear stress, τ_i, as

$$\tau_i = \mu\sigma_r \qquad (2.12)$$

where μ is the coefficient of friction, generally between 0.1 and 0.6.

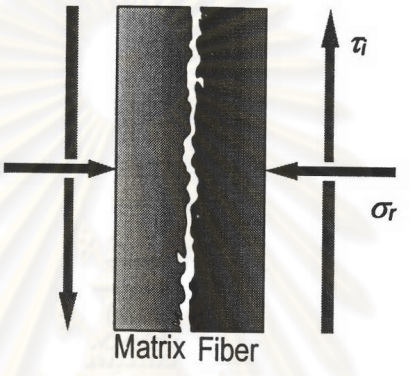

Figure 2.10 Mechanical gripping due to radial shrinkage of a matrix in a composite more than the fiber on a cooling from a high temperature [redrawn form ref. no. 12, p.110].

In general, mechanical bonding is a low-energy bond vis-à-vis a chemical bond, i.e., the strength of a mechanical bond is lower than that of a chemical bond. Pure mechanical bonding alone is not enough in most cases. However, mechanical bonding could add, in the presence of reaction bonding, to the overall bonding. Also, mechanical bonding is efficient in load transfer when the applied force is parallel to the interface. In the case of mechanical bonding, the matrix must fill the pores and surface roughness of the reinforcement. Surface roughness can contribute to bond strength only if the liquid matrix can wet the reinforcement surface. Otherwise the matrix is unable to penetrate the asperities on the fiber surface, it will solidify and leave interfacial void, as shown in Figure 2.11.

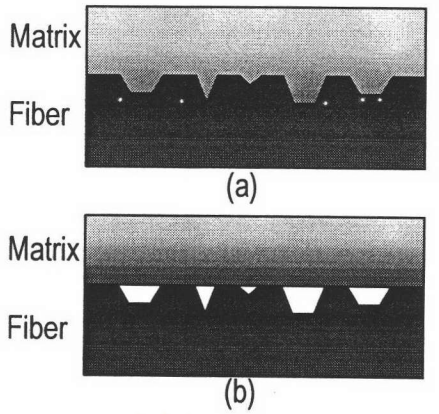

Figure 2.11 a) Good mechanical bond b) Lack of wettability can make a liquid polymer or metal unable to penetrate the asperities on the fiber surface, leading to interfacial voids [redrawn form ref. no. 12, p.110].

2.7.2.2 Physical Bonding

Any bonding involving weak, secondary or van der Waals forces, dipolar interactions, and hydrogen bonding can be classified as physical bonding. The bond energy in such physical bonding is approximately 8-16 kJ/mol. In the case of electrostatic bonding, it occurs when the surfaces carry net electrical charges of opposite sign. Electrostatic forces are unlikely to constitute the major adhesive bond in a composite and they can readily be reduced, for example, by discharging in the presence of a strongly polar solvent, such as water.

2.7.2.3 Chemical Bonding

Atomic or molecular transport, by diffusion processes, is involved in chemical bonding. Solid solution and compound formation may occur at the interface, resulting in a reinforcement/matrix interfacial reaction zone with a certain thickness. Chemical bonding involves primary forces and the bond energy in the range of approximately 40 - 400 kJ/mol. There are two main types of chemical bonding:

a. *Dissolution bonding*: In this case, interaction between components occurs at an electronic scale. Because these interactions are of rather short range, it is important that the components come into intimate contact on an atomic scale. This implies that surface should be removed any impurities. Any contamination of fiber surfaces, or entrapped air or gas

bubbles at the interface, will hinder the required intimate contact between the components.

b. *Reaction bonding*: In this case, a transport of molecules, atoms, or ions occurs from one or both of the components to reaction site, that is, the interface. This atomic transport is controlled by diffusional process.

Two polymer surfaces may form a bonding owing to the diffusion of matrix molecules to the molecular network of the fiber, thus forming tangled molecular bond at the interface. For example, Figure 2.12(a) shows the diffusion of free chain ends at the interface between two polymers, which leads to chain entanglements and a rise in the adhesive strength. This effect is employed in some coupling agents used on fiber in thermoplastic matrices. The adhesive strength is dependent on the nature of the resultant interatomic bonds (and also on the stresses generated by the reaction – see below).

Various types of chemical reaction may occur at the interface, either deliberately promoted or inadvertent. These can be represented, as in Figure 2.12(b), by new A-B bonds being formed as a result of interfacial chemical reactions. These bonds may be covalent, ionic, metallic, etc., and in many cases are very strong. There are many examples of the interfacial bond strength being raised by localized chemical reactions, but it is often observed that a progressive reaction is occurred which results in the formation of a brittle reaction product [6, p.135-136].

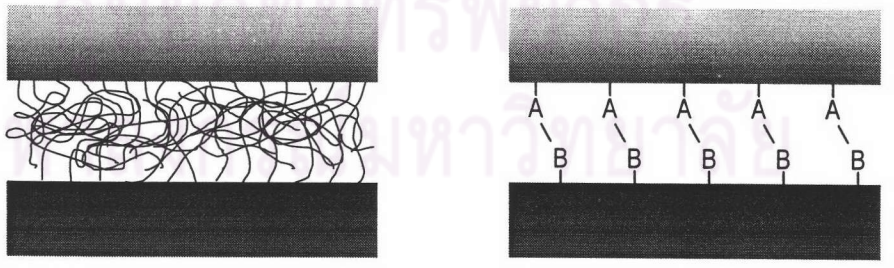

(a) (b)

Figure 2.12 Interfacial bonds formed by (a) molecular entanglement following interdiffusion and (b) chemical bonding.

2.7.3 *Optimum Interfacial Bond Strength*

Two general ways of obtaining an optimum interfacial bond involve fiber or reinforcement surface or matrices modification. It should be emphasized that maximizing the bond strength is not always the goal. In brittle matrix composites, too strong a bond would cause embrittlement. The situation can illustrate by examining the following three cases.

a. *Very Weak Interface or Fiber Bundle (No Matrix)*

This extreme situation will prevail when there is no matrix and the composite consists of only a fiber bundle. The bond strength in such a composite will only be due to interfiber friction. A statistical treatment of fiber bundle strength shows that the fiber bundle strength is about 70 to 80% of average single-fiber strength.

b. *Very Strong Interface*

The other extreme in interfacial strength is when the interface is as strong as or stronger than the higher-strength component of the composite, generally the reinforcement. In this case, of the three components – reinforcement, matrix and interface – the interface will have the lowest strain failure. The composite will fail when any weak cracking occurs at a weak spot along the brittle interface. Typically, in such a case, a catastrophic failure will occur, and the resulted composite will have very low toughness.

c. *Optimum Interfacial Bond Strength*

An interface with optimum interfacial bond strength will result in a composite with enhanced toughness, but without a severe penalty on the strength parameters. Such a composite will have multiple failure sites, most likely spread over the interfacial area, which will result in a diffused global spread of damage, rather than a vary local damage.

2.8. Polymer Surface

2.8.1 Differences between Polymer Surface and Bulk

Even for a pure linear homopolymer thermoplastic there are potential differences between the surface and the interior (bulk or average). Polymer chains have end-groups which may be functionally quite different from the repeating unit (especially if they result form the incorporation of initiating and termination species used during the polymerization process). The chains are characterized by a molecular weight distribution and for certain polymers (e.g. polyamides) very low molecular weight oligomers may be present preferentially as cyclic, rather than linear species. Many polymers are semicrytalline, possessing regions which are microcrystalline and regions which are amorphous. End- groups tend to be excluded from crystallites; they may even confer surface activity. In principle, therefore, the homopolymer surface may differ from the bulk in end-group concentration, molecular weight distribution and amorphous:crystalline ratio. Deviations from complete linearity of the polymer chain arising from branching or cross-linking introduce additional complexity.

Copolymers have increased potential for surface:bulk differentiation, particularly in the case of block and graft copolymers. Here there is a tendency for like sections of the polymer structure to associate and the possibility that one component may dominate the surface region. Polymer blends (or alloys) represent this effect *in extremis*, since few polymers are actually compatible.

For thermoset polymers, with their extended three dimensional cross-linked network structure, the situation is somewhat simplified. Nevertheless, the cross-link density at the surface may differ from that of the bulk due to preferential segregation of either prepolymer or cross-linking agent (or catalyst if used), or too poor component mixing.

There are numerous possibilities for the unintended presence of additives or contaminants at the surface. Since surface behavior can be markedly affected by them, these unintended molecules are generally regarded as 'surface contamination'. Contamination by direct contact is often unavoidable and even deliberate, e.g. in the application of sizes and finishes in fiber production or in the spraying of molds with releasing agents.

2.8.2 Depth Scales Associated with Surface Behavior

In the case of polymers, the transition from surface to bulk properties would take place over length scale of the order of polymer chain sizes, i.e. up to several tens of nanometers, leading to less stringent sampling depth requirements. For some properties this is certainly true, but it does not necessarily follow that polymer surface phenomena are governed by the structure and composition within these same dimensions. In general, surface is not a well-defined term. A *surface* defined by one surface analysis technique may be the bulk as defined by another technique.

2.9 Polymer Surface Modification Techniques

Because polymers are inert materials and usually have a low surface energy, they often do not possess the surface properties needed to meet the demands of various applications. For these reasons, surface modification techniques are required, especially in composite application. In recent years, many advances have been made in developing surface treatments to alter the chemical and physical properties of polymer surfaces without affecting buck properties. These treatments have been applied to achieve the following purposes:

- Produce special functional groups at the surface for specific interactions with other functional groups
- Increase surface energy
- Increase hydrophobicity or hydrophilicity
- Improve chemical inertness
- Introduce surface cross-linking
- Remove weak boundary layers or contaminants
- Modify surface morphology by increasing or decreasing surface crystallinity or roughness
- Increase surface electrical conductivity
- Increase surface lubricity

The general requirement to 'surface engineer' polymeric materials has led to the development of many surface modification techniques, as listed in Table 2.4.

Table 2.4 Treatments used to modify plastic surfaces. [14, p.5]

Surface treatment	Effect
Mechanical process	
Sand blasting	cleaning, roughening
Grinding, brushing	roughening
Chemical process	
Solvent wipe	cleaning, roughening
Acid etching	oxidation, roughening
Ozone treatment	oxidation
Coating/grafting	attachment of different polymer chains
Gas-phase fluorination	fluorination
Sodium naphthalenide/THF (for PTFE)	defluorination/oxidation
Physico-chemical Process	
Corona discharge	oxidation
Flame	oxidation
Thermal	surface annealing, oxidation
Inert gas plasma	cross-linking
Active gas plasma	functionalisation
Plasma deposition	cross-linked thin polymer coating
Ion etching	functionalisation, roughening
Laser	cross-linking, oxidation, roughening
UV light	cross-linking, oxidation

Details of some well-known and important methods are briefly discussed as follows.

2.9.1 Corona Discharge Treatment

Corona discharge, which can be obtained with a relatively simple and inexpensive setup, is a popular industrial technique for the surface treatment of continuous polyolefin films. In a corona discharge system, plasma is produced when air is ionized by a high electric field. The atmospheric pressure plasma, which is called corona discharge, causes various chemical and physical changes on polymer surface for improving bondability and printability. Very often, for continuous treatment of films, a corona discharge system is installed downstream of an extruder. A corona treatment system consists of a high-voltage and high-frequency generator, and electrode and a grounded metal roll as shown in Figure 2.13 (a)

2.9.2 Flame Treatment

Flame has been used to treat polyolefin and other polymeric products. The setup-a burner ans a fuel tank- is very simple and portable. However, craftsmanship is needed to produce consistent. Typically, flame treatment produces an oxidized polymer surface for improving bondability with an adhesive or for improving printability and mark permanence. A schematic diagram of the flame treater is shown in Figure 2.13 (b).

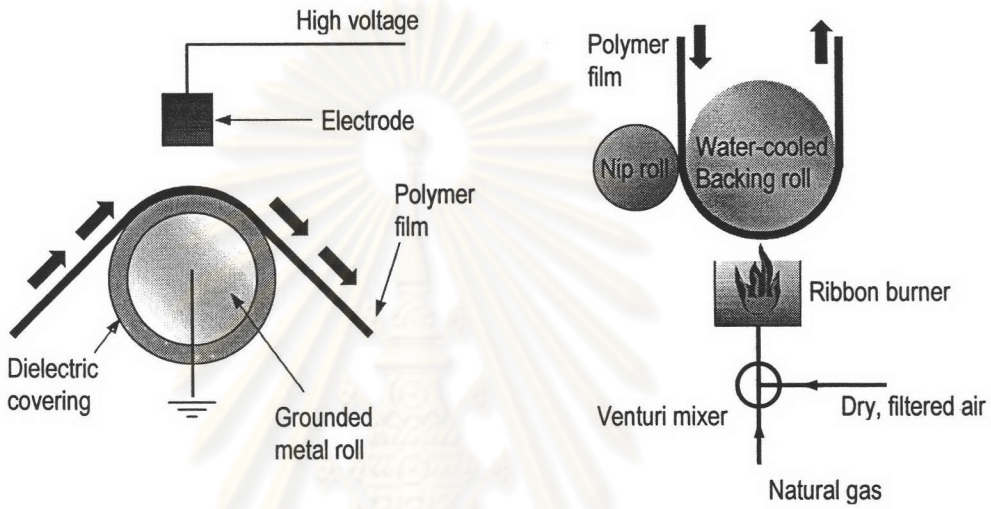

Figure 2.13 Schematic diagrams of (a) corona-discharge and [redrawn from ref 13, p.266] (b) flame setup [redrawn from ref no 15, p.237]

2.9.3 Plasma Treatment

Plasma treatment is probably the most versatile surface treatment technique. Water and different types of gas such as argon, nitrogen, fluorine and carbon dioxide can produce unique surface properties required by various applications. For example, oxygen-plasma treatment can increase the surface energy of polymer, whereas fluorine-plasma can decrease surface energy and improve chemical inertness. Cross-linking at a polymer surface can be introduced by inert gas plasma. Modification by plasma treatment is usually confined to the top several hundred angstroms and does not affect the bulk properties. Surface modified by using plasma can be fairly uniform over the whole surface area. The main disadvantage of this technique is that it requires a vacuum system, which increases the cost of operation. The plasma process is extremely complex and the process parameters are highly system dependent; the optimal parameters developed for one system usually can not be adopted for another system. Moreover, the scale-up to a large production is not simple and it is very

difficult to control precisely the amount of a particular function group formed on surface. A schematic diagram of plasma system is shown in Figure 2.14.

In general, reactions of gas plasma with polymers can be classified as follows:

- *Surface Reactions*: Reaction between gas-phase species and surface species and reactions between surface species produce functional groups and cross-linking, respectively.
- *Plasma Polymerization*: The formation of thin film on the surface of a polymer via polymerization of an organic monomer in plasma.
- *Etching*: Materials are removed from a polymer surface by physical etching and chemical reactions at the surface to form volatile products.

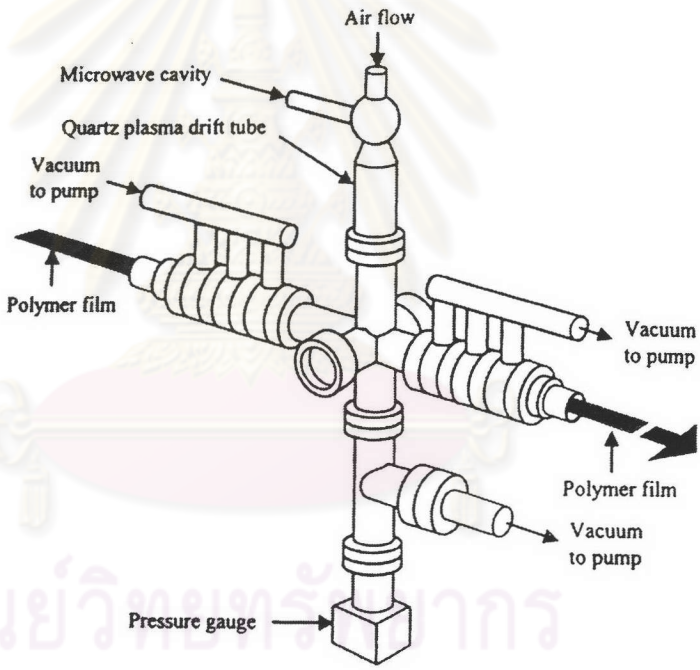

Figure 2.14. Schematic diagram of the remote-plasma treater (not drawn to scale) [15, p.238].

2.9.4 Chemical Treatment

Chemical treatment has been used in industry to treat large objects that would be difficult to treat by other commonly techniques such as flame and corona-discharge treatments. Chemical etchants are used to convert smooth hydrophobic polymer surfaces to rough hydrophilic surfaces by dissolution of amorphous regions and surface oxidation. Etching of a polymer surface is an important step for preparing the polymer surface for electroless

plating and adhesive bonding. The choice of etchants is polymer dependent. Chromic acid is the mostly widely used etchant for polyolefins and other polymers.

In the foregoing examples, the solution interacts strongly with the polymer surface, producing a very diffuse interface. The modification can change only the chemical structure of polymer surfaces, very specific functional groups are introduced on the surface.

2.9.5 Ion-Beam Modification

Ion beams have been used to texturize polymer surfaces, especially fluoropolymers, to increase adhesion. Different types of chemical reaction—reduction, oxidation, cross-linking, ion implanation, loss of heteroatoms and loss of aromaticity via ring opening—have been shown to occur during ion bombardment of polymers. The frequency of these chemical reactions depends on the type of ion used, the nature of the polymer, ion energy, and beam dose. Ion-beam modification of polymers has perhaps been most useful in preparing polymer surfaces for metallization.

2.9.6 Radiation Grafting

Radiation grafting is a very versatile technique by which surface properties of a polymer can be tailored through the choice of different monomers. The most common radiation sources are highly-energy electrons, gamma radiation and ultraviolet and visible light. Grafting is usually performed by irradiating the polymer in the presence of a solvent containing a monomer. Alternatively, grafting can be initiated thermally by contacting the polymer, which has been pre-radiated in air to produce reactive groups on the surface, with a monomer. Systems are available for both batch and continuous modes of operation. Surface photografting can be performed in a vapor or liquid phase, as shown in Figure 2.15.

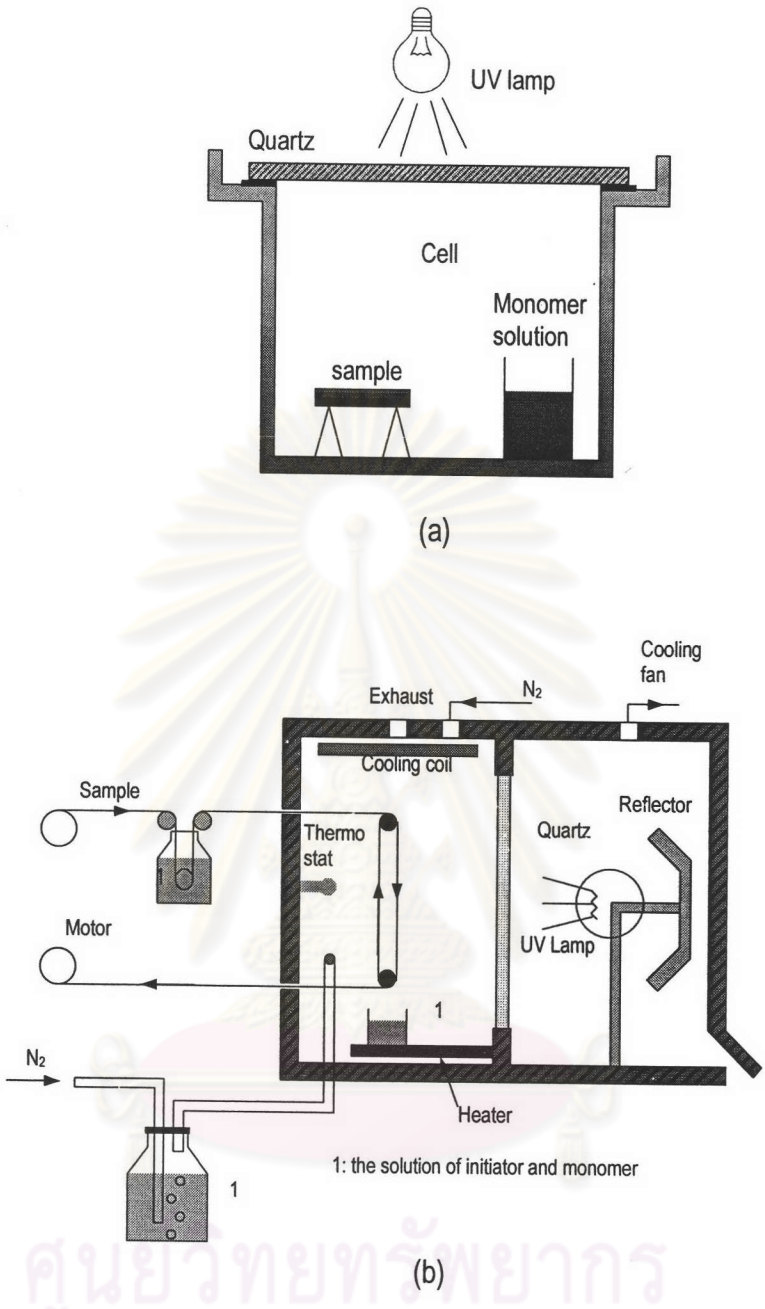

Figure 2.15 Laboratory-scale photo-grafting process by Ranby et. al (a) batch process for polymer films and (b) continuous process for yarns, filaments and film strips [redrawn from 16, p. 305, 312]

2.10 Photo-Oxidation Process as a Polymer Surface Modification Technique

The energies associated with near-ultraviolet radiation quanta are about 3.0-4.3 eV which correspond to 72-97 kcal/mol. Common covalent bonds encountered in polymers have bond dissociation energies which for the most part are either lower or within this energy range [17, p.547]. A photochemical reaction requires that a photon is absorbed to commence the reaction. The excited state thereby populated can then undergo a variety of transitions, which can be classified as photophysical and photochemical processes [18, p.3]. Photophysical processes do not produce new chemical compounds, but interconvert excited states with each other or excites with ground state. Photochemical processes, on the other hand, produce new chemical species which are different from the starting materials.

Provided the ultraviolet radiation is absorbed by the polymer and suitable pathways are available for the photoexcited singlet (S) and triplet (T) species to transfer the absorbed energy to cause photochemical reactions. Unfortunately, in most systems a variety of competing photophysical processes, such as phosphorescence (from ($T_1 \rightarrow S_0$) transition) or fluorescence (from ($S_1 \rightarrow S_0$) transition), may preclude chemical reaction. The photoreactions of polymers tend to involve the triplet excited states of molecules rather than the ground or singlet stage species because of the relatively longer lifetime of the former. The lowest excited triplet state, T_1, is formed by non-radiation intersystem crossing from the lowest excited singlet state, S_1. Higher triplet state can form only from a triplet-triplet absorption where a molecule in the T_1 state absorbs a photon (see Figure 2.16)

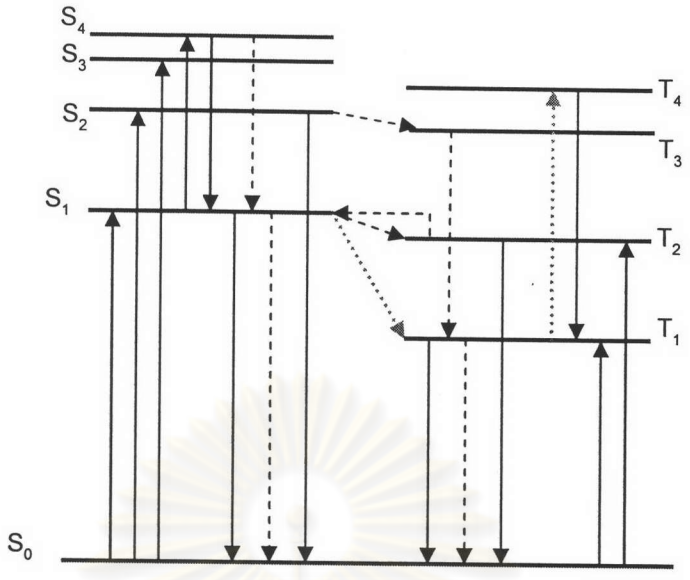

Figure 2.16 Unimolecular photophysical processes. Solid lines: radiative transitions; broken lines: non-radiative transitions. The dotted lines show formation of lowest excited triplet state, T_1 by intersystem crossing (broken line) and its transition to higher triplet state (solid line) [redrawn from 19, p.30].

The absorption process of electromagnetic radiation is a necessary prerequisite for photoreaction. It is convenient to discuss the photoreaction process in terms of three stages: initiation, propagation, and termination. When oxygen presents, photo-oxidation occurs. The photo-oxidation of almost every polymer is summarized in the following schematic [20, p.24]:

Initiation

$$PH,O_2 \xrightarrow{h\upsilon} HO_2^{\bullet},P^{\bullet},H_2O_2$$

$$H_2O_2 \xrightarrow{h\upsilon} 2^{\bullet}OH$$

$$^{\bullet}OH + PH \longrightarrow H_2O + P^{\bullet}$$

Propagation

$$P^{\bullet} + O_2 \longrightarrow PO_2^{\bullet}$$

$$PO_2^{\bullet} + PH \longrightarrow POOH + P^{\bullet}$$

$$HO_2^{\bullet} + PH \longrightarrow HOOH + P^{\bullet}$$

$$PO_2^{\bullet} + PH \xrightarrow{h\upsilon} P^{\bullet} + HO_2^{\bullet} + P^{\bullet}$$

$$HO_2^{\bullet} + PH \xrightarrow{h\upsilon} H^{\bullet} + HO_2^{\bullet} + P^{\bullet}$$

$$PO_2^{\bullet} \xrightarrow{h\upsilon} P^{\bullet} + HO_2^{\bullet}$$

$$PO_2^{\bullet} \xrightarrow{h\upsilon} -C(=O)H + CH_2 = CH - + {}^{\bullet}OH$$

$$(POOH)_s + PH \xrightarrow{h\upsilon} P=O + H_2O + PH$$

$$(POOH)_t \xrightarrow{h\upsilon} P_1 - \underset{\underset{O}{\|}}{C} - R + CH_2 = CH - P_2 + H_2O$$

where $(POOH)_s$ and $(POOH)_t$ are polymeric hydroperoxides secondary and tertiary, respectively

$$(POOH)_t + P_1CH_2CH_2P_2 \xrightarrow{h\upsilon} POH + H_2O + P_1 - CH = CH - P_2$$

$$P=O \xrightarrow{h\upsilon} P_1 - \underset{\underset{O}{\|}}{C}{}^{\bullet} + {}^{\bullet}CH_2 - P_2$$

$$P=O \xrightarrow{h\upsilon} P_1 - \underset{\underset{O}{\|}}{C} - CH_3 + CH_2 = CH - P_2$$

Termination

$$PO_2^{\bullet} + PO_2^{\bullet} \longrightarrow P=O + P-OH + O_2$$

$$PO_2^{\bullet} + HO_2^{\bullet} \longrightarrow \begin{cases} POOH + O_2 \\ P=O + H_2O + O_2 \end{cases}$$

$$HO_2^{\bullet} + HO_2^{\bullet} \longrightarrow HOOH + O_2$$

These steps can be discussed in details as follows.

1. Initiation step: This first step is formation of free radicals. Polymer (PH) containing intra-molecular chromophoric groups and/or light absorbing impurities (RH) (inter-molecular impurities) can produce radicals in the presence of oxygen under UV/VIS (visible) irradiation:

$$PH \xrightarrow{h\upsilon(O_2)} P^{\bullet} + HO_2^{\bullet}$$

$$RH \xrightarrow{h\upsilon(O_2)} R^{\bullet} + HO_2^{\bullet}$$

$$PH + R^{\bullet} \longrightarrow P^{\bullet} + RH$$

where $P^{\bullet}$ = polymer alkyl radical and $HO_2^{\bullet}$ = hydroperoxy radical. Hydroperoxy $HO_2^{\bullet}$ radicals can react with each other to produce hydrogen peroxide (H_2O_2), which can be further photolysed into hydroxyl radicals ($HO^{\bullet}$), which in turn can react with polymer (PH) to produce polymer alkyl radicals ($P^{\bullet}$).

2. Propagation step: In this sequence there are reactions of free polymer radicals with oxygen to produce polymer oxy- and peroxy-radicals and secondary polymer radicals which resulting in chain scission. The key reaction of propagation step is the formation of polymer peroxy radicals ($POO^{\bullet}$) by the reaction of polymer alkyl radicals ($P^{\bullet}$) with oxygen:

$$P^{\bullet} + O_2 \rightarrow POO^{\bullet} \qquad (2.13)$$

This reaction is very fast but diffusion-controlled. The next propagation step is the abstraction of a hydrogen atom by the polymer peroxy radical ($POO^{\bullet}$) to generate a new polymer alkyl radical ($P^{\bullet}$) and polymer hydroperoxide (POOH).

$$POO^{\bullet} + PH \rightarrow P^{\bullet} + POOH \qquad (2.14)$$

The propagation step is very much dependent on the efficiency of the decomposition (photolysis and/or thermolysis) of polymer hydroperoxides (POOH) during which new radicals such as polymer oxy radical ($PO^{\bullet}$) and hydroxyl radical ($HO^{\bullet}$) are formed:

$$POOH \xrightarrow{h\upsilon \text{ or } \Delta} PO^{\bullet} + {}^{\bullet}OH \qquad (2.15)$$

Polymer oxy radicals ($PO^{\bullet}$) and very mobile hydroxyl radicals ($HO^{\bullet}$) abstract hydrogen from the same or from a nearby polymer (PH) chain:

$$PO^{\bullet} + PH \rightarrow POH + P^{\bullet} \qquad (2.16)$$

$$HO^{\bullet} + PH \rightarrow P^{\bullet} + H_2O \qquad (2.17)$$

Polymer oxy radicals ($PO^{\bullet}$) undergo a number of other reactions (considered as chain branching reaction), including:

a. β-scission reactions which result in fragmentation of the polymer chain together with formation of end carbonyl (or end aldehyde) groups and end polymer alkyl radicals:

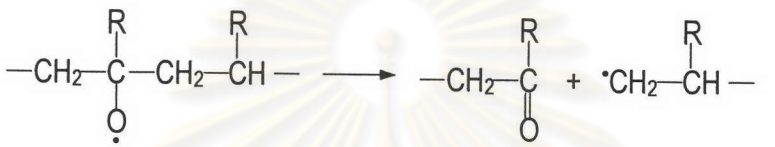

(2.18a)

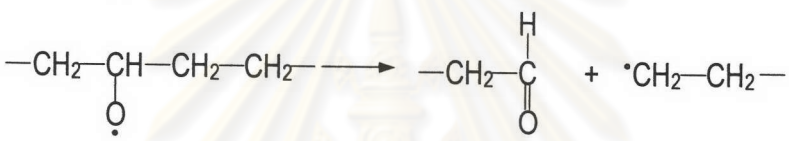

(2.18b)

Formation of in-chain ketone groups:

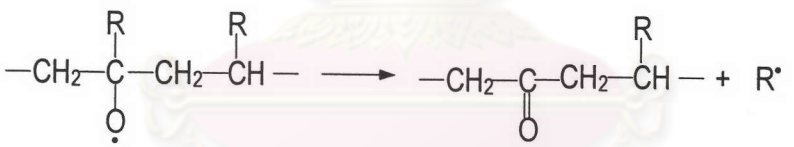

(2.19)

Radical induced hydroperoxide decomposition:

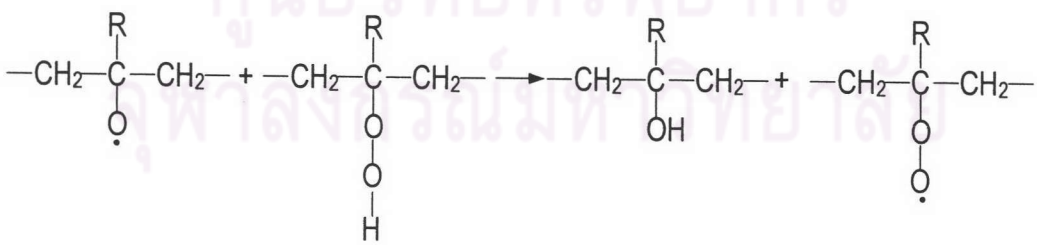

(2.20)

d. Reaction between two polymer alkoxy radicals producing simultaneously a carbonyl and hydroxyl group by disproportionation:

(2.21)

Formed ketonic (CO) groups plays a very important role in further mechanisms of oxidation of polymers.

3. Termination step: The termination of the polymer radicals occurs by bimolecular recombination:

$$P^{\bullet} + P^{\bullet} \longrightarrow P\text{—}P \qquad (2.22a)$$

$$P^{\bullet} + PO^{\bullet} \longrightarrow POP \qquad (2.22b)$$

$$P^{\bullet} + POO^{\bullet} \longrightarrow POOP \qquad (2.22c)$$

$$PO^{\bullet} + PO^{\bullet} \longrightarrow POOP \qquad (2.22d)$$

$$PO^{\bullet} + POO^{\bullet} \longrightarrow POOOP \longrightarrow POP + O_2 \qquad (2.22e)$$

$$POO^{\bullet} + POO^{\bullet} \longrightarrow POO\text{—}OOP \longrightarrow POOP + O_2 \qquad (2.22f)$$

Termination reactions also occur between low molecular radicals such as hydroxyl ($HO^{\bullet}$) and hydroperoxy ($HO_2^{\bullet}$) and other available radicals ($R^{\bullet}$):

$$P^{\bullet} + HO^{\bullet} \longrightarrow POH \qquad (2.23a)$$

$$P^{\bullet} + HO_2^{\bullet} \longrightarrow POOH \qquad (2.23b)$$

$$P^{\bullet} + R^{\bullet}(H^{\bullet}) \longrightarrow PR \text{ (or } PH) \qquad (2.23c)$$

$$PO^{\bullet} + HO^{\bullet} \longrightarrow POOH \qquad (2.23d)$$

$$PO^{\bullet} + HO_2^{\bullet} \longrightarrow POH + O_2 \qquad (2.23e)$$

$$PO^{\bullet} + R^{\bullet}(H^{\bullet}) \longrightarrow POR \text{ (or } POH) \qquad (2.23f)$$

$$PO_2^{\bullet} + HO^{\bullet} \longrightarrow POH + O_2 \qquad (2.23g)$$

$$PO_2^{\bullet} + HO_2^{\bullet} \longrightarrow POO\text{—}OOH \longrightarrow POOH + O_2 \qquad (2.23h)$$

$$PO_2^{\bullet} + R^{\bullet}(H^{\bullet}) \longrightarrow POR \text{ (or } POH) \qquad (2.23i)$$

When the oxygen pressure is high (atmospheric pressure), the termination reaction almost exclusively occurs by reaction in Equation 2.22d. At low oxygen pressure other termination reaction take place to some extent. The termination reaction of two polymer alkyl radical $P^{\bullet}$ (Equation 2.22a) occurs mainly in vacuum.

2.10.1 Photo-oxidation of Polymers by Oxygen Reactive Species [20, p.399-409]

2.10.1.1 Ozone

Being an endothermic allotrope of oxygen, ozone (O_3) may serve as a precursor for reactive oxygen species such as atomic oxygen (O) and singlet oxygen $^1O_2$. The absorption of light by ozone consists of three bands: 200-320 nm (Hartley band), 300-360 nm (Huggins band) and 440-850 nm (Chappuis band). The primary photochemical processes differ considerably in each of these bands. The quantum yield of ozone photolysis at 254 nm is almost unity. The main photoproducts are atomic oxygen (O) and singlet oxygen $^1O_2(^1\Delta_g)$, according to the reaction:

$$O_3 \xrightarrow{h\nu} O(^1D) + {}^1O_2(^1\Delta_g) \quad (2.24a)$$

$$O(^1D) + O_3 \longrightarrow 2O + O_2 \quad (2.24b)$$

$${}^1O_2(^1\Delta_g) + O_3 \longrightarrow O + 2O_2 \quad (2.24c)$$

Upon exposure of polymers to ozone and light, four active species, i.e. ozone itself, atomic oxygen, singlet oxygen and molecular oxygen may simultaneously react with the polymer, which causes ozone-ozonization to proceed by complicated mechanisms and kinetics (Figure 2.17). Low concentrations of ozone are able to cause severe oxidation and cracking of many polymers such as polyolefins, polystyrene, polyvinyl chloride) and rubbers, even without light. In many cases, ozone accelerates the photodegradation of polypropylene, 1,2-polybutadiene and etc.

Ozone can react with saturated hydrocarbon (RH) in reactions in which hydrogen abstraction is followed by rehybridization of the carbon atom from sp^3 to sp^2 state:

$$RH + O_3 \longrightarrow R^\bullet + {}^\bullet OH + O_2 \longrightarrow ROO^\bullet + {}^\bullet OH \quad (2.25a)$$

$$ROO^\bullet + RH \longrightarrow ROOH + R^\bullet \quad (2.25b)$$

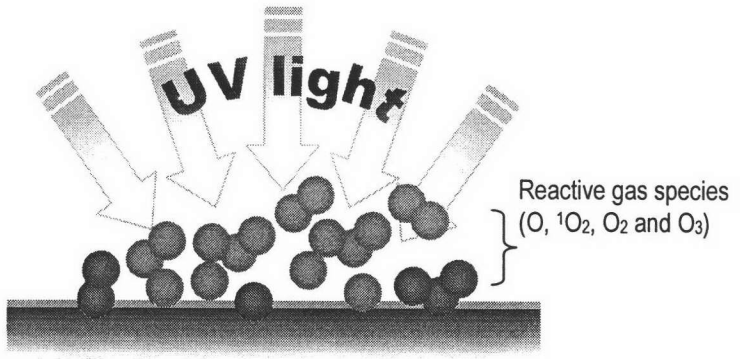

Figure 2.17 The schematic represents reaction mechanism on polymer surface by reactive gas species (ozone, atomic oxygen, singlet oxygen and molecular oxygen) under UV irradiation.

Similar reactions occur in the ozonation of polyolefins. Polymer alkyl radicals formed during ozonation of polypropylene react immediately with molecular oxygen to form polymer peroxy radicals ($POO^{\bullet}$). The reaction rates and concentrations of intermediate polymer peroxy radicals are proportional to the surface area and to the square root of the ozone concentration.

Hydroxyl radicals ($HO^{\bullet}$) formed in reaction 2.25a can react with polymer alkyl radicals ($P^{\bullet}$) to form a polymer hydroxyl group (reaction 2.26a) or abstract hydrogen with the formation of double bonds in the polymer chain (reaction 2.26b).

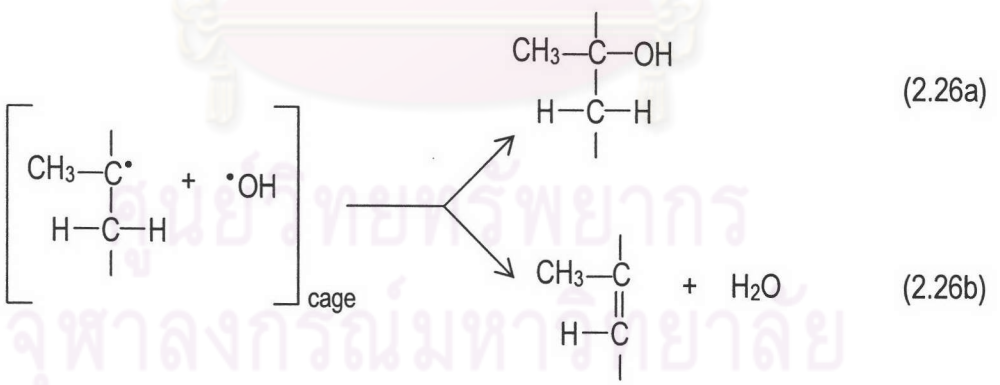

(2.26a)

(2.26b)

The double bonds react with ozone to form an unstable π-complex, which rapidly decomposes to a switterion and an aldehyde or ketone group:

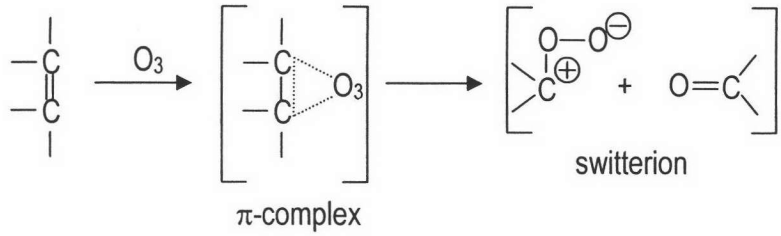

(2.27)

In further reactions corssozonide, dimeric peroxide, carboxylic or ester groups can be formed according to the following mechanisms:

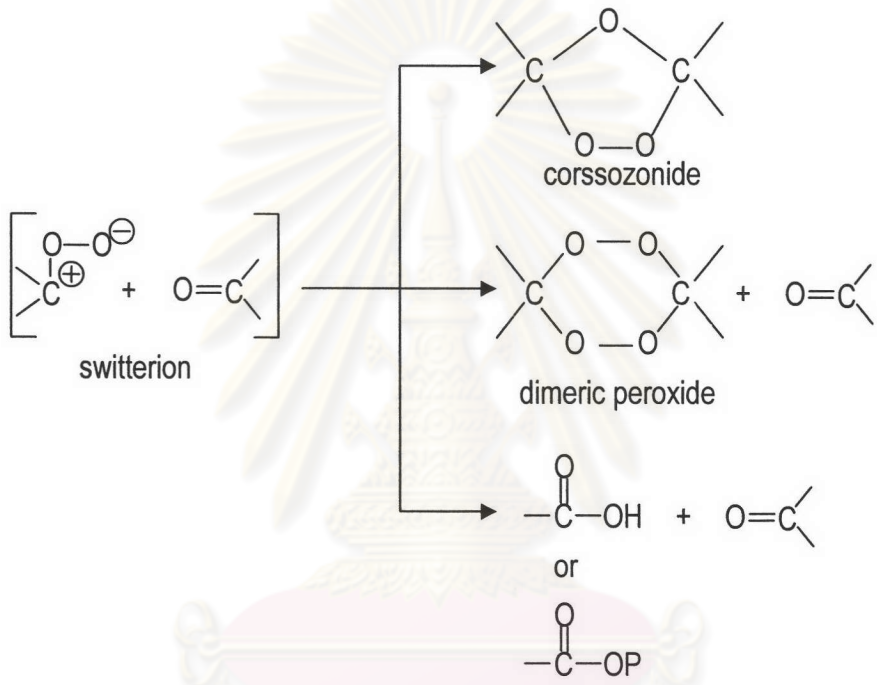

(2.28a)

(2.28b)

(2.28c)

2.10.1.2 Atomic Oxygen

The main products of ozone photolysis are atomic oxygen $O(^3P, ^1D, ^1S)$ and singlet oxygen $^1O_2(^1\Delta_g, ^1\Sigma_g^+)$. Atomic oxygen $O(^3P)$ is the main source of singlet oxygen:

$$O(^3P) + O(^3P) \longrightarrow {}^1O_2 \qquad (2.29)$$

$$O(^3P) + O_3 \longrightarrow {}^1O_2 + O_2 \qquad (2.30)$$

Atomic oxygen reacts rapidly with several polymers. Figure 2.18 shows the effect of atomic oxygen on the weight loss of different polymers. Highly branched polymer such as polypropylene and polymer with ether links, e.g. poly(oxymethylene), are most readily attacked by atomic oxygen. Perfluorinated polymers, rubber vulcanized with sulphur and highly aromatic polymer are the most resistant. Oxidation of polymers by atomic oxygen occurs only at or near the surface of the polymers. For that reason, the elucidation of the reaction mechanisms and reaction kinetics is very difficult.

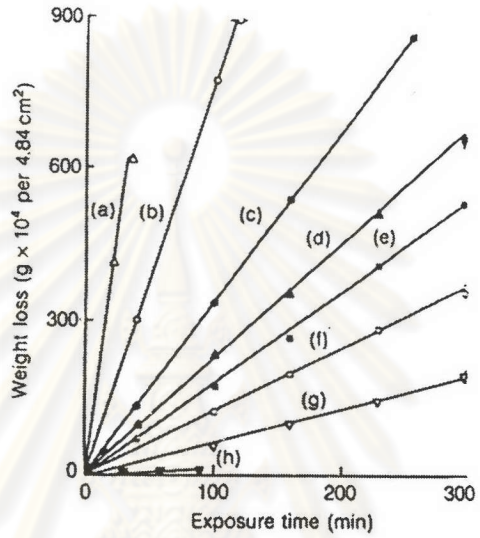

Figure 2.18 Relative effect of atomic oxygen on different polymers: (a) polysulphides; (b) polyformaldehyde; (c) polypropylene; (d) low density polyethylene; (e) poly(ethylene glycol terephthalate); (f) polystyrene; (g) polytetrafluoroethylene and (h) sulphur-vulcanized natural rubber. [20, p.403]

2.10.1.3 Singlet Oxygen

Isolated molecules of singlet oxygen, $^1O_2(^1\Delta_g)$, at low pressure undergo a spontaneous transition to the ground state ($^3\Sigma_g^-$), which has a half-life of 45 min. The role of singlet oxygen in the photo-oxidation of polymers is mainly limited to those photosensitized oxidation process in which singlet oxygen can be produced. Photosensitized oxidation involves photochemical excitation of the sensitizer (S) to its singlet excited state (^1S), intersystem crossing to the triplet state (^3S), energy transfer to the ground state oxygen (O_2) and subsequent reaction of the resulting $^1O_2$ with a given polymer (acceptor) (PH) to yield the products of oxidation (POOH):

$$S \longrightarrow {}^1S \longrightarrow {}^3S \qquad (2.31a)$$

$${}^3S + O_2 \longrightarrow S + {}^1O_2 \qquad (2.31b)$$

$${}^1O_2 + PH \longrightarrow POOH \qquad (2.31c)$$

Many organic compounds, especially dyes are efficient photosensitizers for singlet oxygen ($^1O_2$) generation. However, the mechanism of dye photosensitized reaction of polymers not only involves the singlet oxygen oxidative mechanism, but also various free radical processes, the formation of oxygen radical ions and other oxygen reactive species, and it is very complex. It is generally accepted that singlet oxygen can react with polymers which contain unsaturated bonds as elements of their structures e.g. polydienes, or in the form of abnormal structures (internal impurities), e.g. polyolefins and poly(vinyl chloride). Many polymers react with singlet oxygen ($^1O_2$), depending upon the reaction conditions, $^1O_2$ oxidation of polymers may be accompanied by extensive degradation and/or crosslinking.

2.10.2 Photo-oxidation of Poly(ethylene terephthalate)

Poly(ethylene terephthalate) are thermally stable, but photometal ions play a significant role in the rate of photoreaction. The latter may be particularly important, since metal derivatives are used as either transesterification or polycondensation catalysts during the manufacturing process. Poly(ethylene terephthalate) film transmits radiation of wavelength > 320nm, but absorbs strongly near 310 nm, and is opaque to radiation of weave length < 302 nm (Figure 2.19).

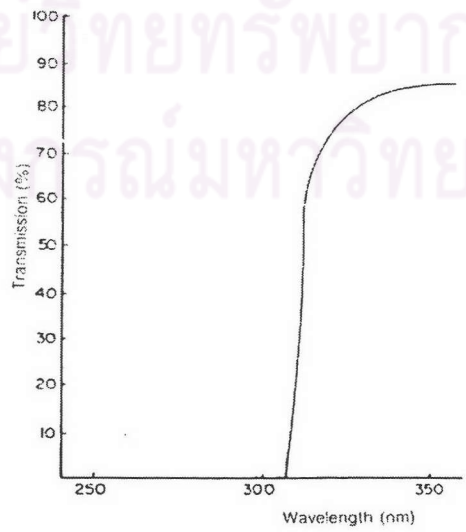

Figure 2.19 Transmission spectrum of poly(ethylene terephthalate) [20, p.289]

The UV irradiation of poly(ethylene terephthalate) causes random chain scission by:

1. the Norrish Type I mechanism:

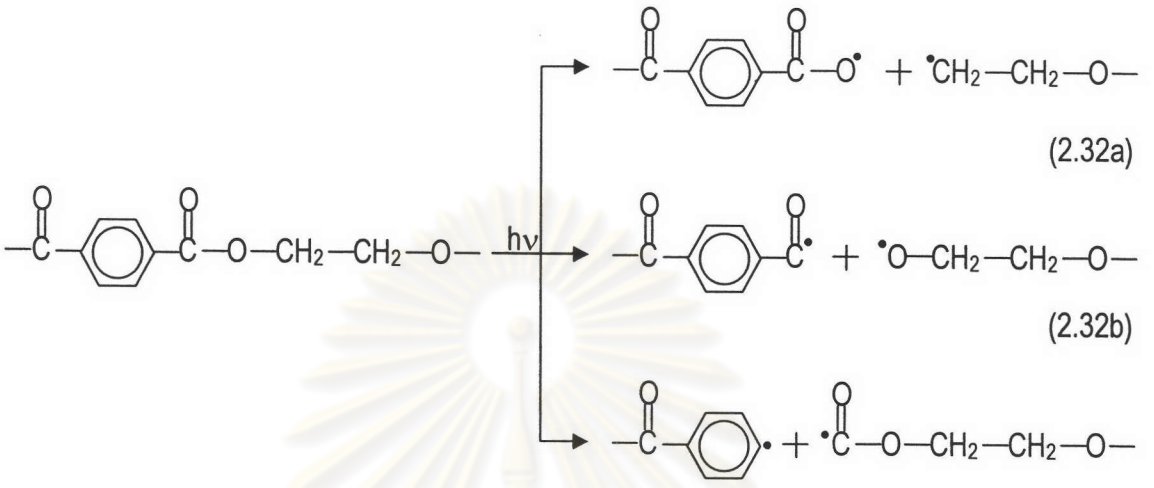

(2.32a)

(2.32b)

(2.32c)

2. and alternatively by Norrish Type II cleavage:

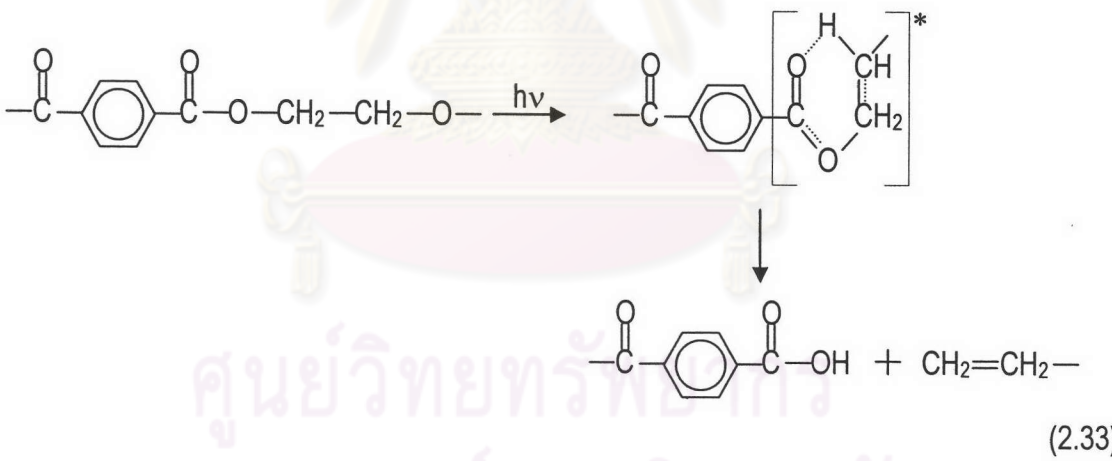

(2.33)

Carbon monoxide and carbon dioxide are produced by the reactions:

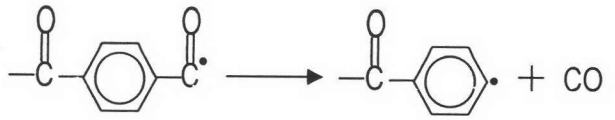
(2.34a)

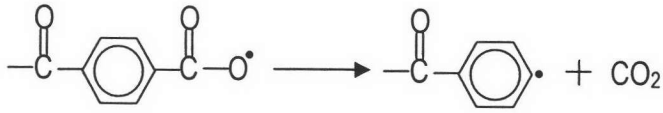
(2.34b)


(2.34c)


(2.34d)

The rate of evolution of carbon dioxide is much higher in the presence of air. The quantum yields of CO and CO_2 formation are 6×10^{4} and 2×10^{-4} respectively, and they have the same values when a sample is exposed to 253.7 and 313 nm irradiation.

The formation of hydroxy and carboxylic end-groups, which are located mainly at the surface, was proved by FTIR-ATR spectroscopy:


(2.35a)

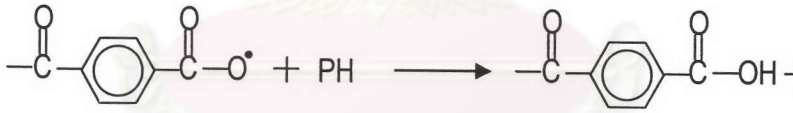
(2.35b)

Hydroxyl groups have also been found to arise as a consequence of substitution reactions in the aromatic ring, resulting in the formation of mono and di-hydroxyterephthalate units:

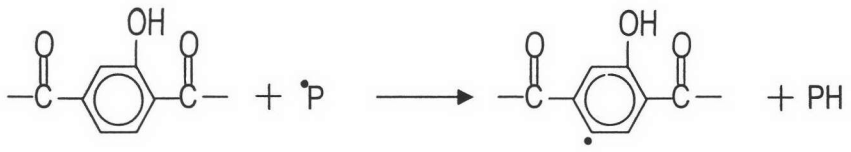

(2.36a)

Mono-hydroxyterephthalate

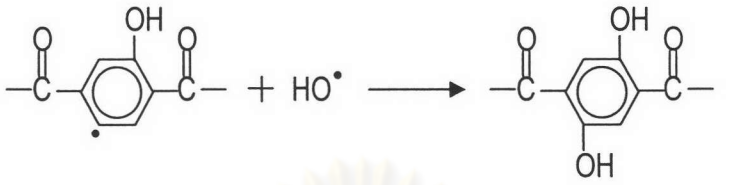

(2.36b)

di-hydroxyterephthalate

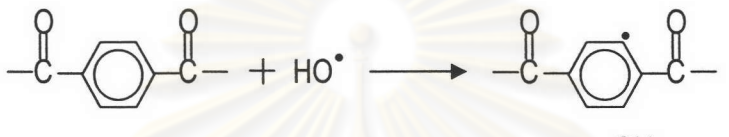

(2.36c)

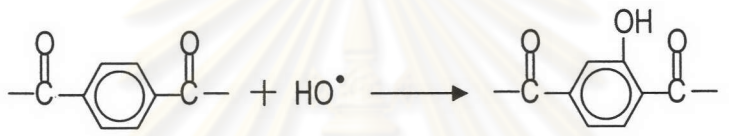

(2.36d)

An alternative mechanism for the formation of mono- and di-hydroxyterephthalate groups is by the formation of benzene ring hydroperoxides:

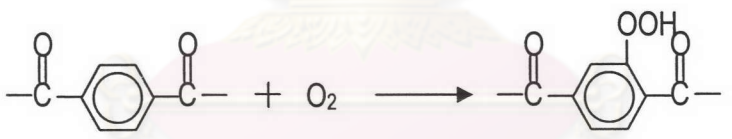

(2.37a)

(2.37b)

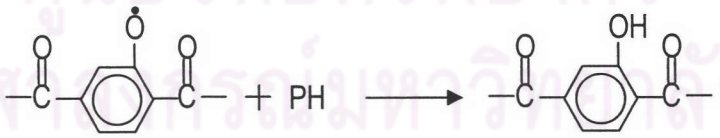

(2.37c)

Commercial polyesters containing both unsaturated and aromatic groups in the chemical chain are crosslinked by the addition of styrene, which reacts with some of the chain double bonds. Chain scission reactions are always accompanied by crosslinking, which causes polymer films to become brittle with crazed surfaces, whereas fibers lose their tenacity, elongation and elasticity. The quantum yield of crosslinking is 5.5×10^{-4}. The crosslinking occurs by termination of all possible polymeric radicals formed during photo-oxidation of the polymer.

2.11 Pultrusion

Being the only common continuous composite manufacturing technique, pultrusion is the most cost-effective of all methods for mass-producing composites. Despite essentially being limited to components with constant cross-section, pultrusion is a fast-growing manufacturing technique and pultruded composites are used in a wide variety of fields spanning every conceivable applications from electrical and civil engineering to sports and medicine [21, p. 250-251]

Pultrusion is distinct from filament winding in that filament winding places the primary reinforcement in the circumferential (hoop) direction whereas pultrusion has the primary reinforcement in the longitudinal direction. Pultrusion is similar to extrusion except that the raw materials are pulled rather than pushed though the die. The process is ideal for high throughput of constant-cross-section products [22, p.98].

The pultrusion process can produce solid, open-sided, and hollow shapes. Almost any length of product is possible. Material utilization is reported to be nearly 95% compared with 75% with hand lay-up. Accurate resin content can be maintained because of the fixed cross-section of the die. As long as the fiber volume passing through the die is constant, excess resin is squeezed out and returned to the resin bath. Inserts made of wire, wood, or foam are readily encapsulated on a continuous basis.

The pultrusion process is continuous, manufacturing 1.5 -60 m/h depending on the shape. The machine may be utilized 24 h a day, 7 days a week, with the only scheduled stoppage required to perform routine cleaning. The operation of a pultrusion machine places severe constraints on the raw material and resin mixture combinations that can be used. The continuous nature of the process also creates opportunities and constraints for the quality control system to be utilized in a pultrusion operation.

In essence, pultrusion is a technique by which continuous fibrous reinforcement is impregnated with a resin and then is continuously consolidated into a solid composite. While there are several different ways to achieve impregnation and consolidation, Figure 2.20 illustrates the different steps in a basic pultrusion step, while Figure 2.21 shows a production facility.

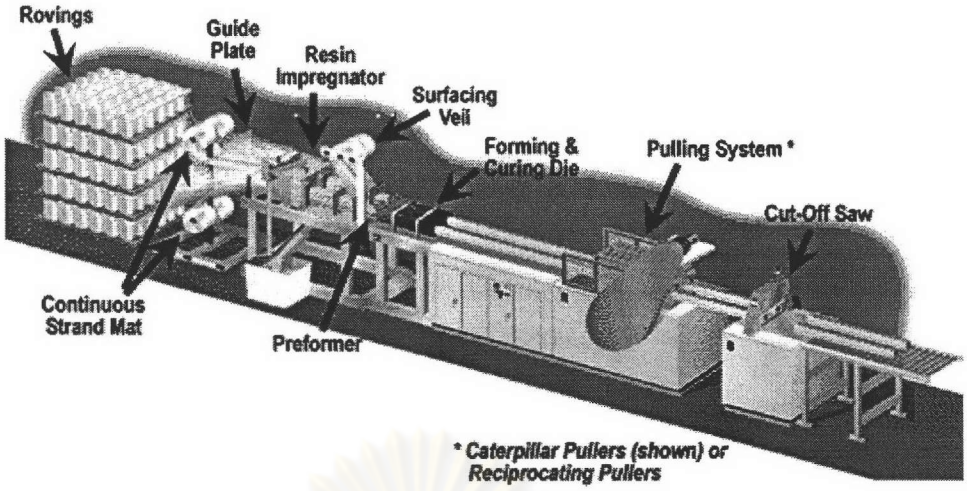

Figure 2.20 Schematic of pultrusion process [23]

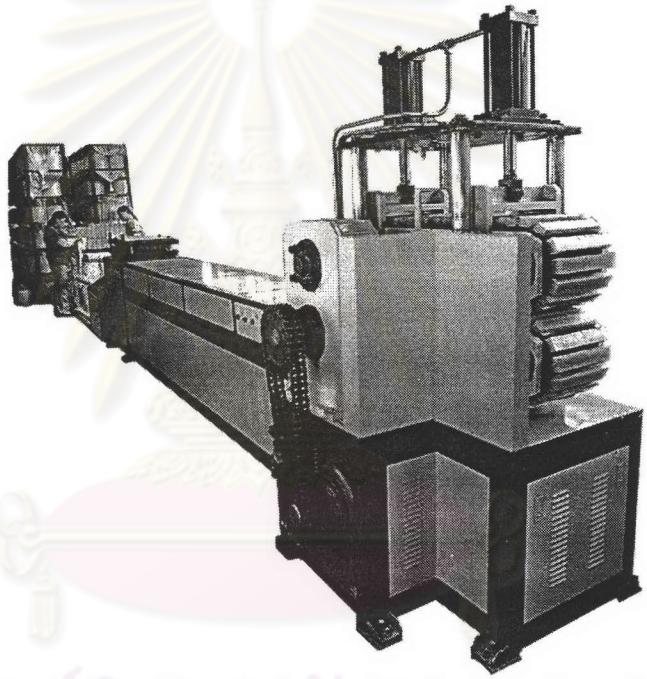

Figure 2.21 Pultrusion facility. From background to foreground; creels (reinforcement supply), guidance devices, impregnation station, die, and caterpillar pullers [24].

A pultrusion machine can be conceptually divided into five basic functional areas of operation with each area performing a special task. The five basic functional areas are listed and described as follows.

Material Feed. The pultrusion yields high strength laminates, but the maximum strength for the shape is attained only when all reinforcements are properly placed in the composite. The process tooling must be engineered to guide the reinforcement into the designed positions within the shape.

The material feed system for wet resin impregnation consists of a bookshelf-style creel with a capacity for 100 or more packages of roving materials. Multiple thread guides or drilled card plates of steel or plastic are used to maintain alignment and minimize fiber breakage. Figure 2.22 shows reinforcement racks.

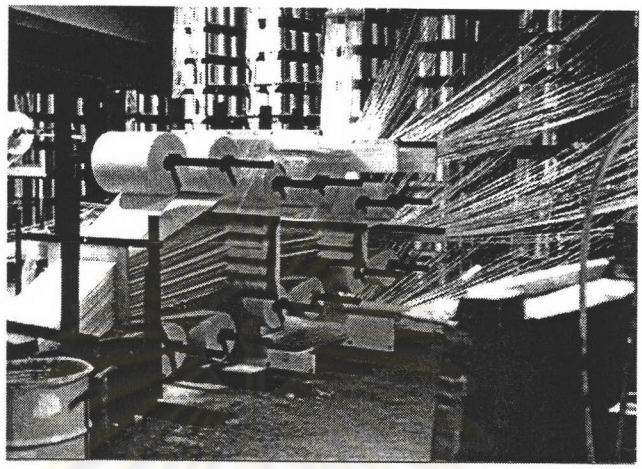

Figure 2.22 Reinforcement racks and creels [24].

Resin Impregnation and Forming. Saturation of the reinforcements with the resin mixture is as important as correct fiber placement. Failure to achieve full impregnation of the reinforcements can produce a pultruded shape with lower mechanical properties than intended. Resin impregnation is achieved by pulling dry fibers through a resin bath equipped with mechanical rollers and wet-out bar to ensure that the fibers are wetted. It is also possible to form dry fibers to shape first then impregnate the shaped fibers by directly injecting resin into the forming die. In the preforming area, preformers are guides that gently and gradually bend the impregnated reinforcements to form the shape being pultruded.

Curing. One of the most challenging steps in the pultrusion process is the continuous polymerization process that take place in the die. Dies may be electrically heated or heated with hot oil. Probably the most widely known method for curing pultruded component is the tunnel-oven process. The reinforced resin is gelled in the die and fully cured in the free state as it pass through a tunnel oven to produce the desired end product. The curing process is always the rate-determining step in the pultrusion process. Curing time is controlled by the curing technique, type of resin, and thickness of the part. For polyester resin parts that are 1-76 thick, typical pultrusion rates are 0.6-1 m/min. Examples of pultrusion dies and preformer were shown in Figure 2.23.

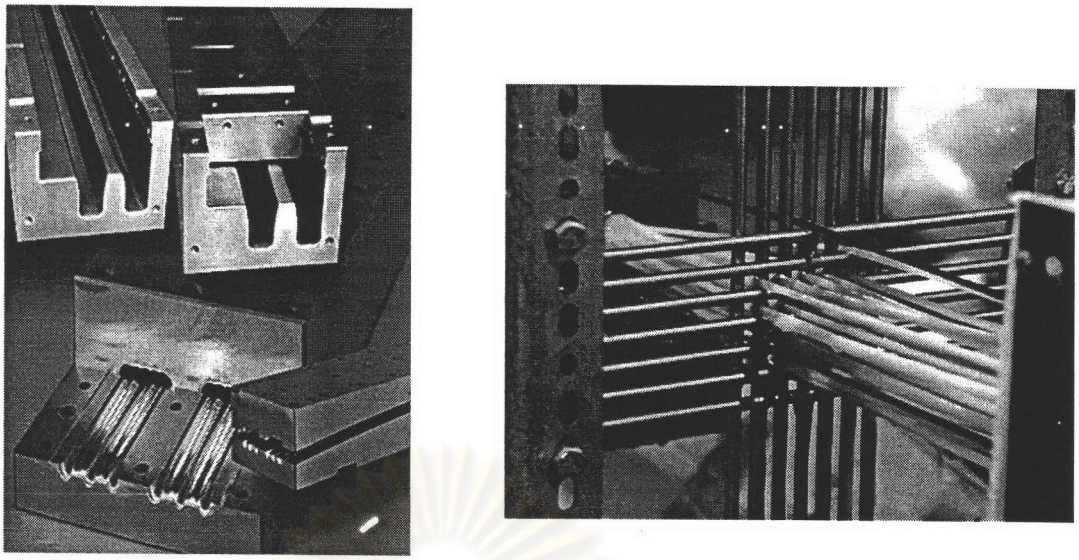

(a) (b)

Figure 2.23 Examples of pultrusion (a) dies and (b) preformer [24].

Pulling Mechanism. The die is separated from the pulling mechanism by a long section to ensure that the consolidated composite can have enough time to be cooled off and gripped by the time it reaches the pulling mechanism, see Figure 2.21. Caterpillar belt pullers are common. The rubber wheels or pads that grip the composite are tailored to fit the specific geometry of the composite, thus reducing the lateral pressure needed to grip the composite, and hence decreasing the risk of crushing a hollow component.

Cutting-off. Since pultrusion is a truly continuous manufacturing technique, composites may be produced in any length that can be handled. Nevertheless, the composite is normally cut. Cutting of the pultrusion product is usually done with either a wet or a dry saw.

From only 20 pultruders producing 10 million pounds of product in 1970 to over 100-120 pultruders producing well over 200 million pounds of product in 1995, it is understandable why the pultrusion market and pultrusion applications have grown. Because of their precise orientation and construction of the various forms of reinforcements, pultrusion has penetrated a large number of application markets e.g. building construction, automotive, aircraft, and etc. A small selection of pultruded profiles that show the range of size and complexity is shown in Figure 2.24.

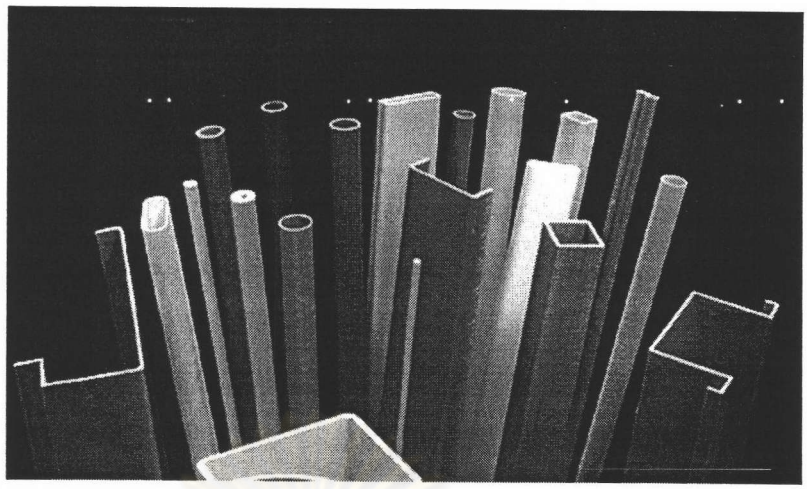

Figure 2.24 Commercial profile designs have unlimited versatility.

2.12 Epoxy Resin

The epoxy resins (also widely known as epoxide resin and, occasionally, as ethoxyline resins) are characterized by the possession of more than one 1,2-epoxy group () per molecule. This group may lie within the body of the molecule but is usually terminal. The three-membered epoxy ring, also called oxirane or glycidyl group, is highly strained and is reactive to many substances, particularly with proton donors, so that reactions of the following schematic form can occur:

(2.38)

Such reactions allow chain extension and/or cross-linking to occur without the elimination of small molecules such as water, i.e. they react by a rearrangement polymerization reaction type of reaction. In consequence these materials exhibit a lower curing shrinkage (3%) than many other types of thermosetting plastics. This means that minimum pressures are required for the fabrication technique normally used on these materials. The shrinkage is much less than that encountered in vinyl polymerizations (8%) used to cure unsaturated polyester resin. This means reduced stress in the cured product. Furthermore, knowledge of the chemistry involved permits the user to cure over a wide range of temperatures and to control the degree of crosslinking. The latter plays an important role in the physical properties [25, p.1-3].

The non-epoxy part of the molecule may be aliphatic, cycloaliphatic or highly aromatic hydrocarbon or it may be non-hydrocarbon and possibly polar. It may contain unsaturation. Similar remarks also apply to the chain extension/cross-linking agents so that cross-linked products of great diversity may be obtained. In practice, however, the commercial scene is dominated by the reaction products of bis-phenol A and epichlorohydrin which have some 80-90% of the market share [26, p.697-698].

Epoxy resins are usually two-part systems, consisting of an epoxy and a curing agent. The epoxy largely dictates the properties of the resin and the curing agent determines the curing temperature. The glass transition temperature of resin is controlled by both components. Most formulations have more than one type of epoxy and more than one curing agent, and are further complicated by numerous other additives that modify curing kinetics, viscosity, and toughness.

In this work, we present here a brief outline of epoxy reactions with amines curing agent. The following description is applicable to aliphatic, cycloaliphatic, and aromiatic amines, but not describes anhydrides or catalytic types of curing agent.

The epoxy chemical group reacts with the amine chemical group as shown in Equation 2.39 [27, p.119-138]. Notice that the hydrogen of the amine group transfers to the oxygen of the epoxy. The amine hydrogens that transfer are called “active hydrogens”. The amine in Equation 2.39 is a secondary amine, which has one active hydrogen. Primary amines have two active hydrogens, and tertiary amines have zero active hydrogen. If both epoxy and amine are difunctional, then linear chain results, as shown in Equation 2.40. If either the epoxy or amine molecule contains higher functionality than two, then a cross-linked resin results. This is shown in Equation 2.41 with a difunctional epoxy and a tetra functional amine.

It is clear from Equation 2.39-2.41 that in epoxy formulations it is desirable to have an equal number of epoxy groups and amine hydrogens.

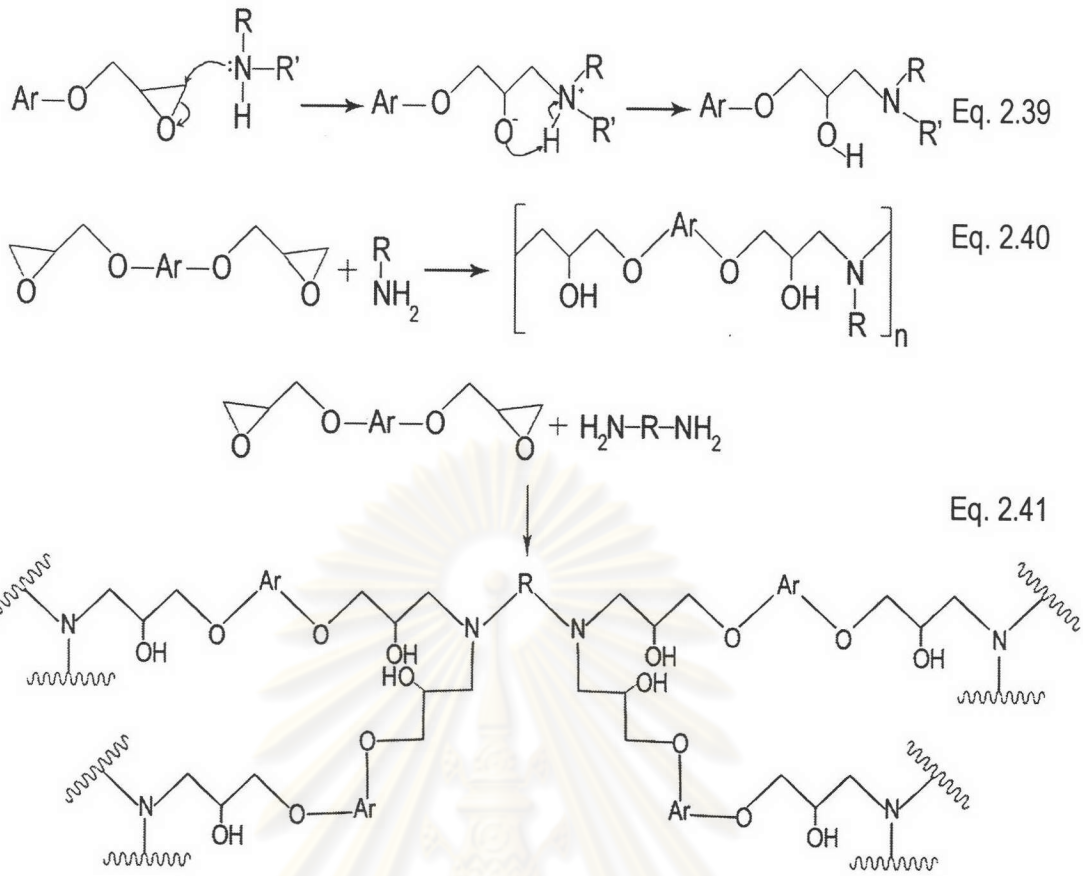

Eq. 2.39

Eq. 2.40

Eq. 2.41

2.12.1 Epoxy Molecules

In spite of the diversity and complexity of the available epoxies, the majority of resins are based on only three epoxy chemistries: TGMDA (tetraglycidyl methylene dianilene), DGEBA (diglycidyl ether of bisphenol A), and phenol formaldehyde novolac epoxy. The major difference between the molecules is that TGMDA and novolacs cures to a higher cross-link density than the bisphenol A epoxy, which leads to higher values of Young's modulus and glass transition temperature but lower values of failure strain.

TGMDA is the major component of the high performance resin formulations. As can be seen in Figure 2.25(a) it is a tetrafunctional epoxy, which results in a high crosslink density after cure. The high cross-link density gives the resin a high value of Young's modulus and a high service temperature. The most objectionable drawback of TGMDA is that the resin's failure strain is low, roughly 1.5%, which leads to large delaminations in composites upon impact, and consequently, low compressive strength after impact. Another problem with TGMDA-based epoxies is water absorption, which occurs because every epoxy amine reaction

results in a hydroxyl group. The hydroxyl groups contribute to the large water absorption, up to 6% of the resin weight.

The bisphenol A-based epoxy (DGEBA), shown in Figure 2.25(b), is the most widely used resin. Compared with TGMDA, bisphenol A epoxy cures to a lower cross-link density. The resin modulus and glass transition temperature are therefore lower, and consequently, the mechanical properties and high temperature performance are also reduced. However, the cured bisphenol A epoxy has a higher failure strain and also lower water absorption.

Numerous other epoxy resins are used in the composites industry in addition to the difunctional bisphenol A epoxy and the TGMDA, a few of which are described below and shown in Figure 2.25 (c) - (f).

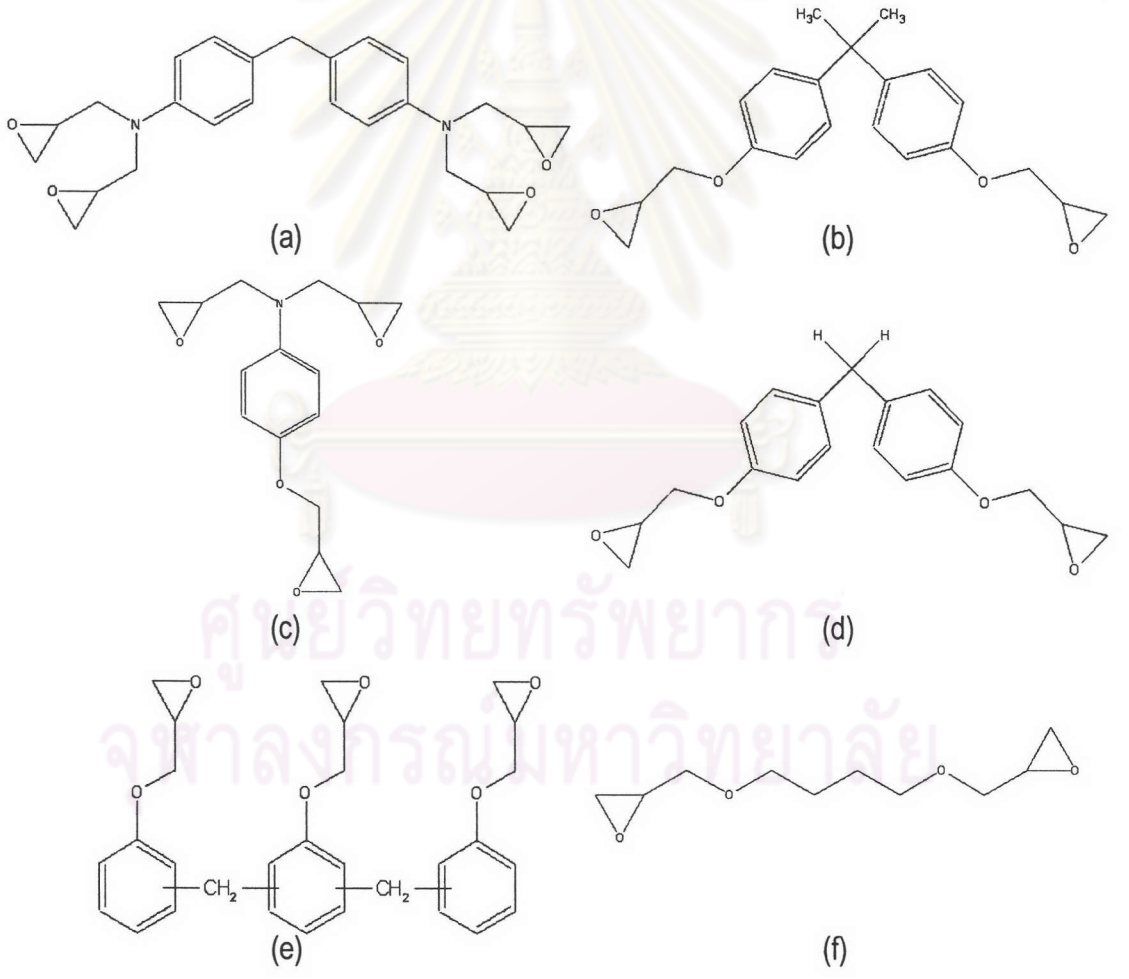

Figure 2.25 The structure of epoxies. (a) TGMDA, (b) DGEBA, (c) Aradite MY 0510, (d) Bisphenol F DGE, (e) Novolac Epoxy, and (f) BDGE.

Novolac epoxies have higher functionality, and consequently cure to a higher cross-link density, than TGMDA. Addition of Novolac to a formulation increases the resin T_g, but decreases the failure stain.

Trifuctional epoxy resins, such as Aradite MY 0510, have properties intermediate between DGEBA and TGMDA. Trifuctional epoxies are used predominantly as a modifier in Prepreg formulations, for example, to increase the failure strain of TGMDA resin or increase the T_g of bisphenol A based epoxy resin.

Bisphenol F epoxy is similar to bisphenol A, differing only in that it has a methylene linkage between aromatic rings instead of the isopropylene linkage in bisphenol A. The advantage of bisphenol F epoxy is that it has a lower viscosity, at 2000-4000 cps, and therefore needs less aliphatic epoxy diluent in formulations that require a low viscosity.

Aliphatic epoxies are used as diluents because they co-cure with the resin and have very low viscosity. Aliphatic epoxies impart a low viscosity to a formulation at the expense of resin T_g. The example shown in Figure 2.25(f) is 1,4-butane diol glycidyl ether (BDGE), which is commonly used because it is difunctional.

2.12.2 Curing Agents

For epoxy resins, a staggeringly large choice of curing agent is available, and these coreactants determine the ultimate thermal and mechanical properties of the resin. Curing agents for epoxies are available with a wide range of cure characteristics, from rapid, room temperature cure to slow cure at 350 °F. The curing agents are of three basic types: amines, anhydrides, and catalytic. Amines are further divided into aliphatic, cycloaliphatic, and aromatic.

2.13 Polyethylene Terephthalate (PET) Fiber

PET fiber is manufactured by the condensation polymerization of two plentiful and inexpensive starting materials, ethylene glycol (an alcohol known to automobile owners as a permanent antifreeze fir radiators, a by product of the petroleum industry) and terephthalic acid (an acid with benzene ring components) [28, p.218]. The process is an ester interchange copolymerization of the ethylene glycol with terephthalic acid itself (Equation 2.42) or with dimethyl terephthalate (Equation 2.43), which results on straight-line molecular units of polyethylene terephthalate as are shown by the following chemical reaction:

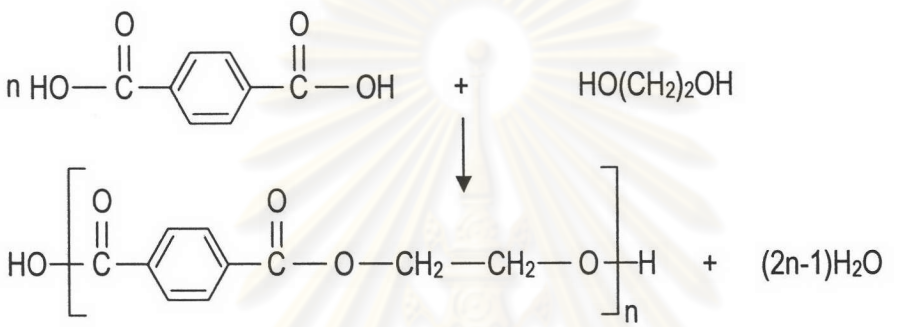

(2.42)

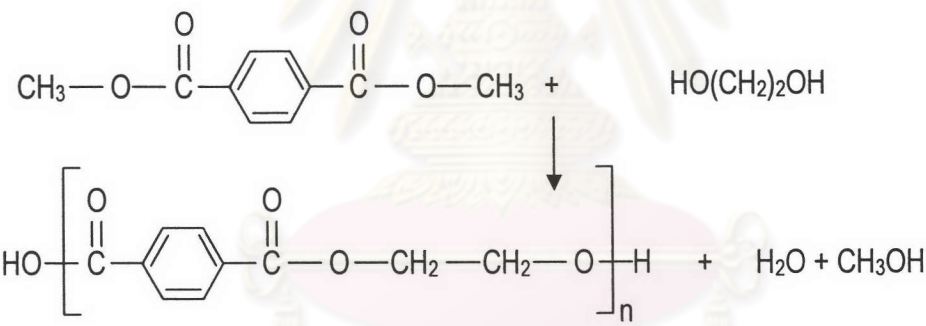

(2.43)

PET fibers have a smooth surface and generally have a circular cross-section, except for some special types produced in trilobal form. PET fiber is produced in a wide range of deniers and staple with bright, semi dull, or dull luster. It has excellent tensile properties, good recovery from stretch, low moisture content and high abrasion resistance [29, p.65]. It has an elongation of 20 to 48 percent. The specific gravity of PET fiber is about 1.38; it has breaking tenacity of 2.8 to 5.2 grams per denier in regular fibers and 6.0 to 9.5 in high-tenacity fibers. PET fiber has good light and weathering resistance. In all practical senses, PET fiber is an inert fiber, highly resistant to most of the common organic solvents. PET fiber is hydrophobic in character. It is more difficult to dye than many fibers, therefore dyed by dyestuffs, such as disperse dyes, and so on, which are insoluble in water.

2.14 Scanning Electron Microscopy/Energy Dispersive X-ray Analysis (SEM/EDX)

Electron microscopes are able to obtain much higher powers of magnification than standard visible light microscopes because electrons have much shorter wavelengths associated with them than light waves. The highest magnification achievable with light microscopes is about 2,000X (times); modern electron microscopes can achieve magnifications approaching 1,000,000X [30].

Scanning electron microscopes (SEMs) use a beam of electrons rather than focused light to form images. The electron beam is scanned across the area to be analyzed in much the same way that the beam is scanned in a television set. The resolution of the SEM is much higher than that of an optical microscope, and images with much greater depth of field are formed.

SEMs have undergone major changes in their capabilities in the past 10 years, owing mainly to the introduction of very bright electron sources. As a result, image resolutions on the order of a few nanometers can be achieved fairly readily, with the ability to detect subtle contrast differences on surfaces. This contrast is what generates the impression of topography in an SEM image [31].

SEM/EDX provides a pictorial representation of the surface with the elemental composition of chosen areas. EDX provides the elemental composition of the surface for elements from boron through uranium. The technique is sensitive for element to approximately 0.1 wt% and can probe depths from 0.2-8 μm depending on the energy of the electron beam used and the average atomic number of the sample [32]. This technique is workhorse of many analyses because of the power inherent in being able to provide a pictorial representation combined with an elemental analysis. With unknown samples, this is frequently the technique of choice for initial analysis. SEM does provide spatial resolution of the surface down to the nanometer range particularly on field emission SEM. With the image, elemental maps of the same area can be acquired to aid in the analysis.

The electron beam used to form the SEM image also generates X-rays, which are characteristic of the elements near the beam. These emitted X-rays can be analyzed to give a composition of the near-surface region. Moreover, X-ray signals may be correlated with the scanning beam to give maps outlining the local elemental concentrations in the near-surface region.

In the SEM, x-rays are produced by accelerating the primary electron beam with enough current to pass through the sample thereby interacting with the elements inner core electrons. When enough high-velocity electron bombardment contacts the innermost electron shell of an atom, it forces the orbiting electron to be kicked out. Subsequently, this results in the neighboring outer electrons to move into the vacant inner electron shell. The release of energy from the escaping electrons from the innermost orbiting shell or core electrons are analyzed and measured based on their classification type. The two types of escaping electrons are classified as either being of low energy or high energy electrons.

The first type of escaping electrons to be discussed are the low energy electrons known as the Auger effect first observed in 1925 by the French Physicist Pierre-Victor Auger. This phenomenon occurs when an electron is released from one of the inner orbiting shells thereby creating two electron vacancies of the residual atom and is repeated as the new vacancies are filled or x-rays are emitted. This type of analysis was developed in the late 1960's and called Auger Spectroscopy or AES. The technique is useful in studying the qualitative and quantitative surface layer composition of compounds, elements, or subatomic particles.

Characteristic x-rays are escaping high energy electrons produced from the bombardment of energetic electrons on the orbiting innermost electron shell of an atom, thereby leaving a vacancy. An electron from the outer orbiting shell then jumps into the empty electron vacant shell. The emitting energy, called a photon or minute energy packet of electromagnetic radiation is specific for each element in the periodic table. The deceleration of the beam electrons when hitting a sample or passing through the field of atomic nuclei is measured and is known as bremsstrahlung or braking radiation. The energy loss is continuous and dependent on the incident electron voltage and angle of incidence.

Figure 2.26 is an illustration of the classical models showing the production of bremsstrahlung, characteristic X-rays, and Auger electrons. In Figure 2.26(a) electrons are scattered elastically and inelastically by the positively charged nucleus. The inelastically scattered electron loses energy, which appears as bremsstrahlung. Elastically scattered electrons are generally scattered through larger angles than are inelastically scattered electrons. In Figure 2.26(b), an incident electron ionizes the sample atom by ejecting an electron from an inner-shell (the K shell, in this case). De-excitation, in turn, produces

characteristic X-radiation (above) or an Auger electron (below). Secondary electrons are ejected with low energy from outer loosely bound electron shells, a process not shown [33].

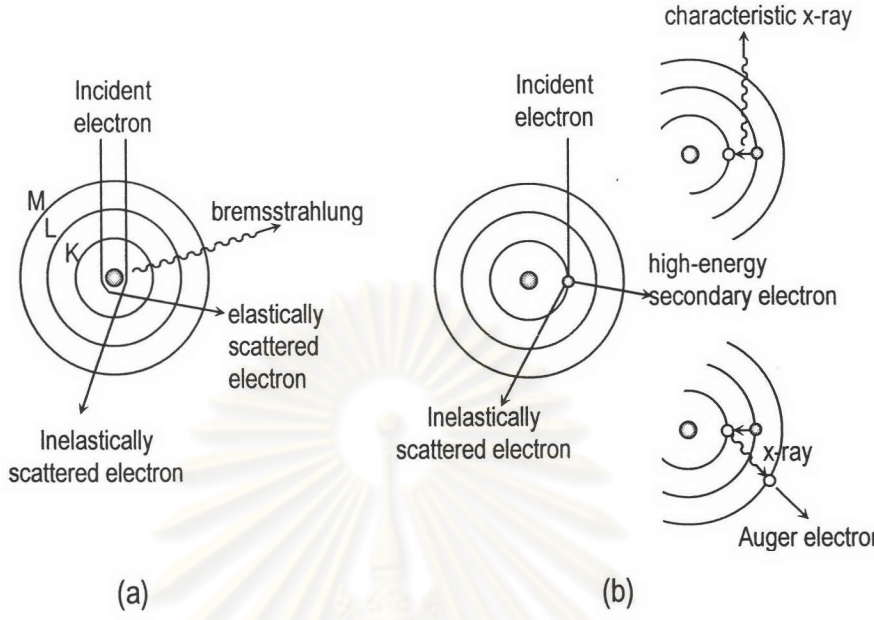

Figure 2.26 An illustration of the classical models showing the production of bremsstrahlung, characteristic X-rays, and Auger electrons.

The detection and measurement of x-rays by scanning electron microscopy is performed by a solid-state detector, also called a semiconductor radiation detector, radiation detector in which a semiconductor material such as a silicon or germanium crystal constitutes the detecting medium. One such device consists of a p-n junction across which a pulse of current develops when a particle of ionizing radiation traverses it. In a different device, the absorption of ionizing radiation generates pairs of charge carriers (electrons and electron-deficient sites called holes) in a block of semiconducting material; the migration of these carriers under the influence of a voltage maintained between the opposite faces of the block constitutes a pulse of current. The sensitivity of these detectors is increased by operating them at low temperatures (commonly that of liquid nitrogen, -164 ºC (-263 ºF)) to suppress the random formation of charge carriers by thermal vibration. Such pulses are amplified, recorded, and analyzed to determine the energy, number, or identity of the incident charged particles. Schematic diagrams showing the components of the energy dispersive system is shown in Figure 2.27. Table 2.5 compares of EDX with some of these practical surface analysis techniques.

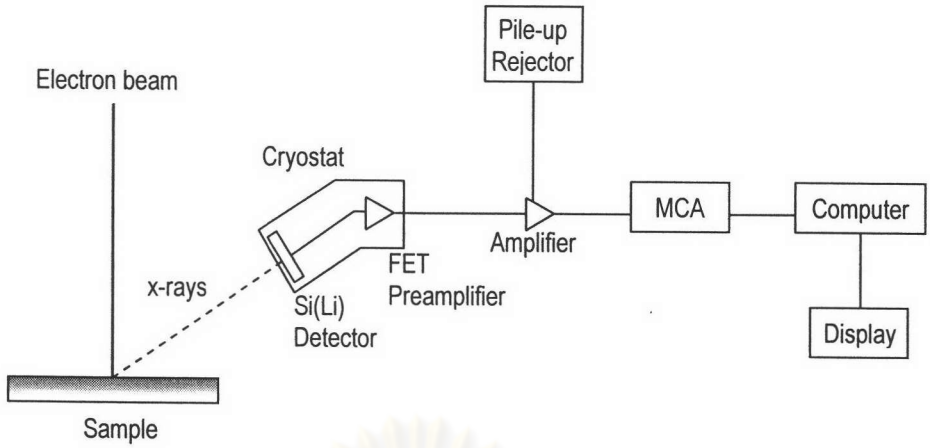

Figure 2.27 Schematic representation of an energy-dispersive spectrometer.

Table 2.5 Compares of some difference surface analysis techniques [34].

	XPS	AES	SIMS	EDX
Vacuum Required	Yes	Yes	Yes	Yes
Incident Particle/Radiation	photon	electron	ion	electron
Emitted Particle/Radiation	electron	electron	ion	photon
Analysis of Emission	energy	energy	mass	energy[1]
Surface Information	Yes	Yes	Yes	No
Elemental Information	Yes	Yes	Yes	Yes
Molecular Information	Yes	(Yes)[2]	Yes	No
Spatial Information	(Yes)[3]	Yes	Yes	Yes
Depth Information	Yes	Yes[4]	Yes	No
Quantitative Information	Yes	Yes	(Yes)[5]	Yes

[1]or wavelength for WDX
[2]limited information can be deduced
[3]typically requires long analysis times
[4]requires auxiliary ion beam etching
[5]with the use of matched standards

2.15 Literature Review

Combinations of ultraviolet light and ozone gas (UVO) have been used for many years to clean organic contaminants from various surfaces. The individual and combined effects of ultraviolet light and ozone on various polymer surfaces, e.g. polyphynylene oxide, polysulphone, polyethylene and polystyrene, were first studied by Peeling and Clark during 1980-1982 [35-37]. Treatment times were of the order of hours in an oxygen atmosphere, resulting in fully oxidized surfaces within the depth sample by X-ray photoelectron spectroscopy (XPS). Peeling and Clark stated that '...the time scale for ozonation and photo-oxidation to produce fully oxidized surfaces is of the order of several hours.' In addition in 1984, Peeling *et al.* also studied the photo-oxidation of poly(ethylene terephthalate) in an oxygen atmosphere at treatment times of up to 30 minutes [38].

In 1988, Rabek *et al.* also studied the effects of ozone and atomic oxygen on polypropylene in the presence of ultraviolet light [39]. Samples were irradiated for 1-8 h in order to characterize the mechanisms of oxidation in weathering situations. Extensive oxidation in these experiments led to embrittlement of the polymer, indicating some effect on the bulk polymer. In 1990, Dasgupta investigated the oxidation of polypropylene and polyethylene in water through which ozone was passed into [40]. While this method has been proved to be an effective technique for modification of polymer for inclusion in wood-pulp blends, the technique has limited applicability.

E. C. Onyiriuka investigated a mechanistic study of high-energy irradiation, e.g. gamma and ultraviolet, in 1992 [41]. The surface chemistry of polystyrene was characterized using angle-dependent X-ray photoelectron spectroscopy (ADXPS), gel permeation chromatography (GPC), infrared spectroscopy, and static secondary ion mass spectroscopy (SIMS). Irradiation of the samples by these high-energy radiation sources led to surface oxidation of the sample to depths greater than 10 nm as opposed to ~3nm depth offered by either plasma and corona-discharge treatment. ADXPS, GPC, and static SIMS data suggested that photodegradation of polystyrene by UV producing carboxyl functionalities as the major products and chain scission was a primary degradation mechanism.

In 1994, T. Yoshikawa *et al.* improved adhesion strength between polyethylene fiber and epoxy resin by exposed the fibers to ultraviolet light in a flow of an oxygen gas containing ozone prior to fabrication of the composite [42]. In the same year, UVO

treatment of poly(ethylene terephthalate) and polypropylene surfaces has been greatly developed by the group of M. Strobel, M. J. Walzak and J. M. Hill [43-45]. A comparative study of gas-phase method, e.g. corona discharge, flame, remote air plasma, ozone and combined UVO treatments was characterized by using X-ray photoelectron spectroscopy (XPS), fourier-transform infrared spectroscopy (FTIR) and contact-angle measurement [43]. The experimental data are in good agreement to those previously reported by Onyiriuka that oxygen incorporated by UVO treatments reach deeper into bulk polymer than the flame, plasma, and corona treatments. In contrast to other techniques, various UVO treatments require orders of magnitude greater exposure time to reach the same levels of surface oxidation. However, the ozone and UVO treatments were done by using a non-continuous batch reactor which was differed from other three methods (flame, remote air plasma, and corona treatments).

M. J. Walzak *et al.* [44] emphasized the study of surface treatments using three different regimes of UV light and ozone: ozone only, UV light in air (producing ozone), and UV light in air supplemented by additional ozone to evaluate the relative importance of ozone, UV light and atomic oxygen, respectively. The duration time needed for modification was found to be between 3 and 10 minutes when the reaction was performed in the presence of ultraviolet light. The reaction mechanisms of polypropylene and poly(ethylene terephthalate) were very different. In the case of polypropylene, if the concentration of reactive species in the gas phase was low, atomic oxygen governed the surface modification, then the radicals generated at the surface and reacted with radicals on other chains to form crosslinked. Poly(ethylene terephthalate) was directly affected by ultraviolet light itself, causing chain scission and modification at the surface regardless of the concentration of the reactive oxygen species.

J. M. Hill *et al.* [45] investigated the stability of polypropylene and poly(ethylene terephthalate) surface-modified using the similar three combinations as M. J. Walzak *et al.*. The results showed that treated poly(ethylene terephthalate) films using these conditions were changed significantly within the first week of aging and washing with water. Conversely, polypropylene changed very little on aging or washing. Low-molecular-weight oxidized material (LMWOM) produced on the polymer surfaces treated with UV/air and UV/air + ozone, was easily removed with water washing. Oxidized groups (carbonyl, carboxyl and hydroperoxide) at the surface of poly(ethylene terephthalate) seemed to migrate in to the bulk. In contrast, the oxidized groups remained at the surface of polypropylene.

In 1995, surface modification of different kind of samples (film, sheet and fiber) of polypropylene and polyethylene by UVO treatment was studied by Hu Xingzhou *et al.* [46]. XPS spectra shown oxygen-containing functional group such as carbonyl, carboxyl and ether were produced after treated with UVO method. Contact-angle measurements, adhesive strength and dyeability of treated sample were also studied. Hu Xingzhou *et al.* concluded that '... UVO treatment was a promising technique to modify polyolefins surface properties'.

Similarly, in 1995, I. Mathieson and R.H. Bradley [47] improved adhesion of polyethylene and polyetheretherketone (PEEK) to epoxy adhesive by UV/ozone surface oxidation. Bond strengths of these polymers to the adhesive were significantly increased after the treatment of one minute, however, at longer exposure times the adhesion level began to deteriorate.

During 1998 to 2000, M. J. Walzak and N. S. Mcintyre *et al.* investigated chemical reactions of the surface of a polypropylene film in the presence of various combinations of UVO methods. In their works, shorter wavelength (184.9 nm) and pulsed UVO treatment and effects of humidity were also studied [48]. They proposed two alternative mechanisms on the oxidation of the polypropylene surface: (1) insertion of an O (^1D) atom to form ether linkages, or (2) hydrogen abstraction by O (^3P), followed either by crosslinking or by reaction with oxygen species to form carbonyl and/or carboxyl functional groups. It was found that reaction (1) dominated initially, but that its rate was reduced by the formation of products from reaction (2). Ether functional groups produced by reaction (1), was primarily responsible for increased surface energy. Carbonyl, carboxyl, and hydroxyl groups formed in reaction (2) appeared to have little effect on surface energy. It was proposed that intramolecular hydrogen bonding of these groups decreasing the availability to increased surface energy. High-energy UV radiation (184.9 nm) was found to play only a minor role in the surface modification of polypropylene. The presence of water vapor during UVO treatment was found to lead to greater oxygen uptake after short-term treatments but did not result in increased surface energy.

This research group also first brought an advanced surface characterization technique, atomic force microscopy (AFM), to examine the changes in morphology and the increase in the adhesion force at the surface of polypropylene after treatment with UVO method [49-50]. It was clearly shown by AFM that UVO treatment resulted in the formation of mounds which arise from the formation of LMWOM. The size of the mounds increased with increasing

treatment time. The adhesion force was estimated from measurement made on the amount of force required to retract the tip from the surface after the two had made contact. A clear increase in adhesion force was observed on the modified polypropylene film surface, which indicated an increase in surface energy of a polymer on a micrometer scale.

In 2000, R. H. Bradley *et al.* [51] investigated the correlation between surface oxygen chemistry and topographical changes of poly(ethylene terephthalate) and polystyrene surfaces by contact-angle measurement, XPS and AFM. Different oxidation mechanisms were proposed for the two polymers. Poly(ethylene terephthalate) appeared to undergo a Norrish-type chain depolymerization reaction, whereas polystyrene was random chain scission attack. AFM analysis showed an increased in the surface roughness with increasing exposure to UVO for both polymers, with grain of LMWOM forming at the surface. This material can be removed by washing, however, complete recovery to the original state was not observed. The XPS results indicated that the point of oxidation was predominantly the ester section of poly(ethylene terephthalate) chain. In both polymers the LMWOM consisted predominantly of carboxylic acid and ester functionalities. Analysis of aged surface showed that for oxidized poly(ethylene terephthalate) surface a relaxation process occurred, lowering the level of surface oxygen. This caused by the diffusion of LMWOM into the bulk, due to its thermodynamically polar nature.

Since UVO treatment is a promising technique to modify polymer surface properties, development of application and apparatus are interested by many research groups. For example, in the year 2000, UVO treatment was applied to improve the mechanical properties of jute-fiber/ epoxy composites, in comparison with corona discharge treatment, by J. Gassan and V. S. Gutowski [52]. Owing to the difficulties in effective treatment of three-dimension objects with corona discharge, the increase of polarity of treated yarns is relatively small, comparing to UVO treatment.

Another example was done by R.H. Bradley *et al.* in 2003 [53]. A fluidized-bed apparatus equipped with UV and oxygen sources had been developed and used for controlled surface oxidative modification of polystyrene microspheres. AFM results showed an increase of the microspheres adhesion which confirmed that UVO method is a suitable method for three dimensional object.